






Additive manufacturing of polymer composites: Sustainability, recycling, life cycle, safety and environmental perspectives

Yasir Beeran Pottathara^{a,*} , Jelena Topić Božič^{a,b} , Simon Muhič^{a,b,c} 

^a Rudolfovo—Science and Technology Centre, Podbreznik 15, Novo Mesto 8000, Slovenia

^b Faculty of Industrial Engineering Novo mesto, Šegova ulica 112, Novo Mesto 8000, Slovenia

^c Institute for Renewable Energy and Efficient Exergy Use, INOVEKS d.o.o., Cesta 2. grupe odredov 17, 1295 Ivančna Gorica, Slovenia

ARTICLE INFO

Keywords:

Additive manufacturing
3D and 4D printing
Polymer composites
Sustainability
Life cycle assessment
Safety and environmental assessments

ABSTRACT

Additive manufacturing (AM) enables the fabrication of complex and customised, on-demand products from various materials across multiple industries in aerospace, automotive, Industry 4.0, and biomedical domains. Advancing material development, improving process efficiency, and ensuring sustainable waste management are crucial for AM to achieve its full capability as a sustainable technology. This review focuses on the recent progress in AM of polymer composites by 3D and 4D printing techniques. Their sustainability, environmental, recycling, lifecycle assessments (LCA), safety, and economic impacts have been systematically reviewed. The effect of incorporating eco-friendly materials in the manufacturing of polymer composites to enable a sustainable future has also been evaluated. The sustainability of additively manufactured polymer composites is evaluated from a social, environmental, and economic perspective. By using recycled materials in the AM processes, the environmental impact can be reduced, circularity promoted, and resources conserved. The challenges of AM techniques regarding scalability, including slow printing speeds, cost limitations, and health and environmental concerns due to the emission of toxic matter and compounds, have been addressed. It also provides a perspective on the potential role of AM in promoting sustainability and circular economic practices for a greener future.

1. Introduction

Additive manufacturing (AM), frequently called 3D printing or rapid prototyping (RP), can be described as a method that constructs layer by layer to produce highly complex structures based on the 3D model data [1]. This technology was introduced in the 1980s by Charles Hull as stereolithography using a computer-aided-design (CAD) tool [2]. Such a layer-by-layer deposition method permits precise control over geometry and material composition at a localised level [3]. While AM has been initially used primarily for prototyping, the technique has evolved into a viable solution for small-scale manufacturing, offering lightweight yet durable parts at a reduced cost. When the CAD tool is combined with computer-aided manufacturing (CAM), AM technologies can shape materials such as polymers, ceramics, metals, and composites into physical objects that closely match their digital designs. The 3D models can be developed using CAD software and mathematical modelling tools, or extracted from medical imaging data, such as magnetic resonance imaging (MRI) or computed tomography (CT). These models are converted into STL files containing information about the object's

surface geometry [4].

AM is widely used for rapid prototyping, where small quantities of a specific part are produced to evaluate design integrity and identify defects, which offers the on-demand production of components at strategically selected locations, which can also reduce shipping costs [5]. AM offers distinct benefits, such as minimised material usage, the capacity to produce intricate and customised geometries, shorter production times, reduced need for centralised inventory, and the capability to repair existing parts. Whereas conventional techniques also have drawbacks, including limited automation, residual stress formation, expensive equipment, complex supply chains, significant inventory needs, limited design flexibility, and increased carbon emissions [6,7]. The ISO/ASTM 52900 standard recognises seven distinct categories of AM technologies: material extrusion, binder jetting, material jetting, directed energy deposition, powder bed fusion, VAT photopolymerization and sheet lamination [8]. The advantages of the AM process make it applicable across a wide range of industries, including aerospace [9–12], automotive [13–15], defense [16–19], biomedical [20–22], orthopaedics [23–26], dental [27–30], fashion [31,32], and the food sector [33–35].

* Corresponding author.

E-mail address: yasir.beeran@rudolfovo.eu (Y.B. Pottathara).

Global environmental issues, particularly in terms of degradability and recycling, can be addressed by AM techniques, which offer a more sustainable prospect by utilising eco-friendly materials, and natural fibre-reinforced materials, resulting in both economic and environmental benefits [36]. The utilisation of such materials slows down climate change and offers sustainable alternatives by reducing waste, improving production conditions and air quality, increasing degradability, and enhancing the possibility of recycling, which leads to a greener modernisation.[37]. This review discusses the incorporation of various polymer composites for AM techniques in terms of their sustainability, recycling, life cycle assessments, safety and environmental effects, commercialization, and economic aspects. We focus on the potential of 3D and 4D printing of polymer composites to enable sustainable solutions across various industries. This review also highlights multiple additive manufacturing processes and their compliance with sustainable conditions. Furthermore, recent advancements in polymer composites for diverse applications will be reviewed. This review also identifies existing challenges in integrating eco-friendly materials and outlines future perspectives for responsible, sustainable innovation and circular economic solutions through additive manufacturing techniques.

1.1. Review methodology

This review deals with the additive manufacturing of polymer composites focusing on the 3D and 4D printing protocols for each AM class. The timespan used for this review is for last five years (from 2020 to 2025) as shown in the flow diagram (Fig. 1). Polymer composites with an emphasis on biodegradable and ecofriendly nature are the focus of this review. Additionally, recycling, life cycle analysis, safety and sustainability, and end-of-life phases of the AM product life cycle are detailed to gain a comprehensive view of the environmental, economic, and social impacts of AM products.

2. Additive manufacturing of polymer composites by 3D printing

Polymers have garnered significant attention in research and applications due to their synthetic versatility, a broad range of processable variants, and the potential to deliver diverse material properties [38].

Despite these benefits, components fabricated solely from pure polymers often lack the mechanical strength and functionality required for structural or load-bearing applications. Composite materials have become a key focus area in recent years in addressing the limitations of pure polymers. Polymer composites are created by combining a polymer matrix with reinforcements to produce properties unattainable by individual constituents alone. These reinforcements can be metallic, ceramic, or polymer-based fibres, whiskers, platelets, or particles, enabling the formation of polymer matrix composites with enhanced structural or functional characteristics. According to ASTM International, AM by 3D (three-dimensional) methods have been categorised into seven: material extrusion, powder bed and ink-jet 3D printing, stereolithography (SLA), direct ink writing or 3D plotting, and direct energy deposition[39]. Each technique has its benefits and drawbacks, and the selection depends on the materials used, processing parameters, cost-effectiveness, and the application of the final product. Fig. 2 illustrates experimental setups for different AM technologies and Table 1 details the recent progress of eco-friendly materials-based polymer composites by 3D printing.

2.1. Material extrusion

Material extrusion is a cost-effective and straightforward processing technique that utilises materials with stable environmental and mechanical properties. The most popular AM techniques in the material extrusion category are fused deposition modelling (FDM) and fused filament fabrication (FFF). In FDM, filaments of thermoplastic polymers are selectively dispensed onto the printing platform through a nozzle, as shown in Fig. 1 (a), according to the CAD file, and no chemical reactions occur during the process. The filaments melt into a semi-liquid state at the nozzle. They are extruded layer by layer onto the printing platform, where layers are fused and then solidify into final parts. The final print can be manipulated by extrusion speed and orientation, layer thickness, and the width and angle of raster [40].

Recently, extrusion-based AM technology has been widely used to fabricate eco-friendly composites for various applications. Eco-friendly composites from Polylactic acid (PLA) and ferronickel slag have been fabricated by the material extrusion [41]. Different concentrations from 2 to14 wt% of ferronickel slag were added to the PLA matrix to produce

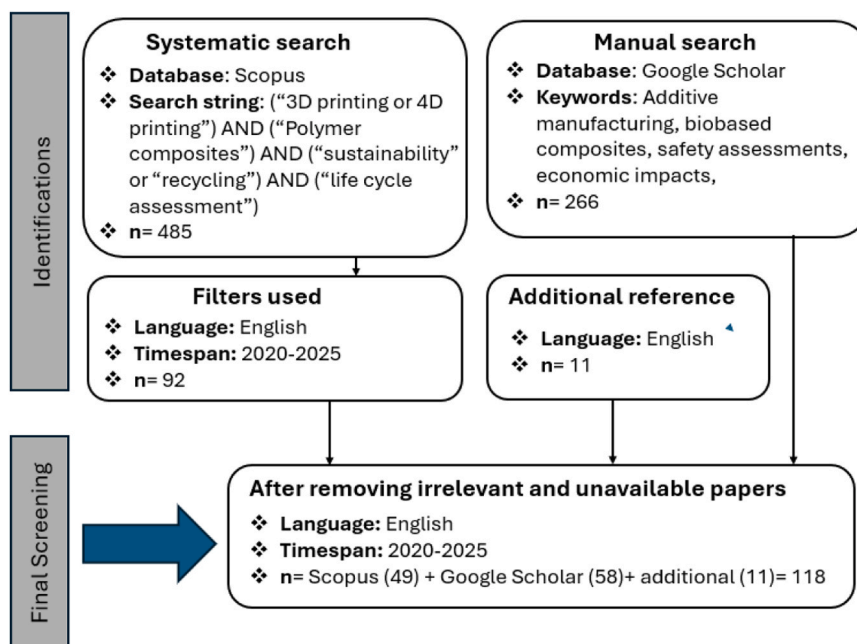


Fig. 1. Flow-diagram of the methodology used in this work.

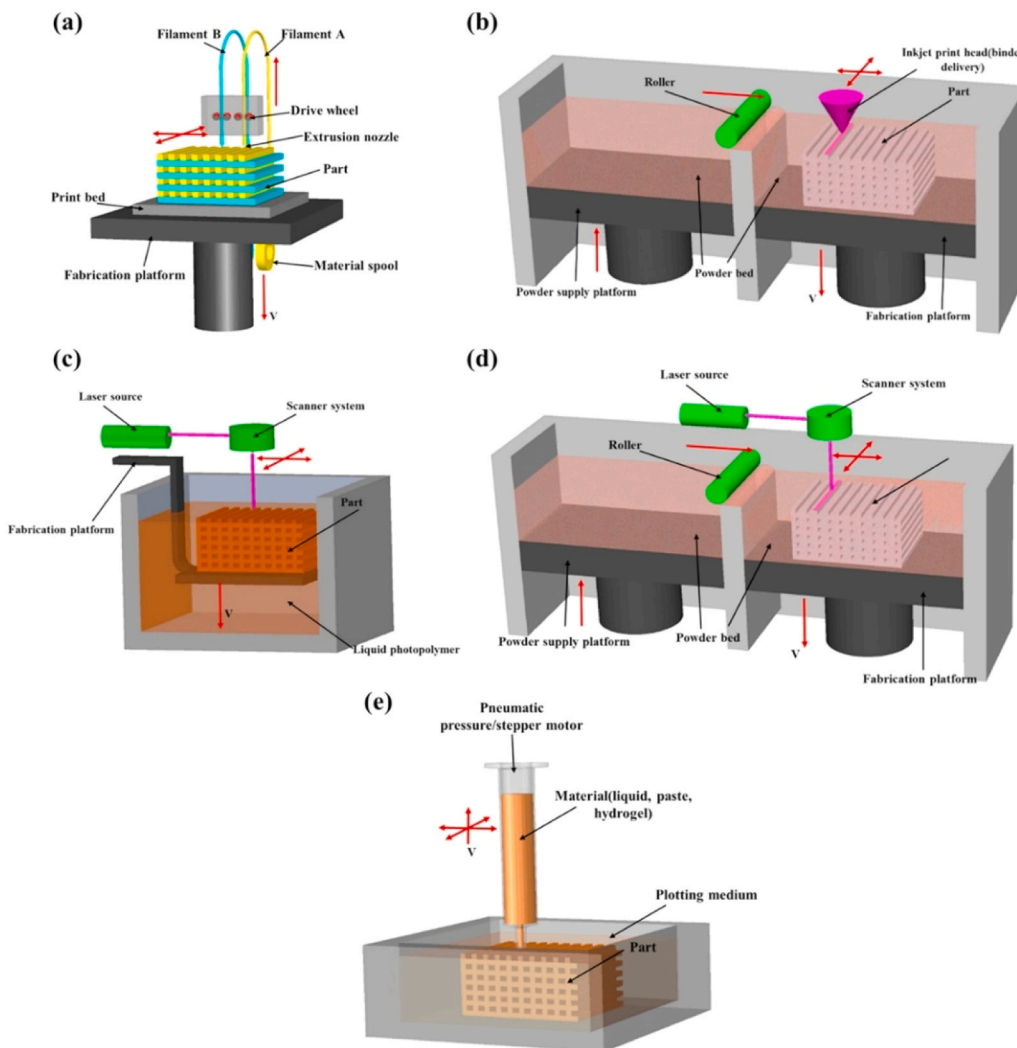


Fig. 2. Schematic illustration of a typical setup for material extrusion through FDM (a), powder bed and inkjet 3D printing (3DP) (b), SLA (c), SLS (d), and Direct ink writing or 3D plotting (e).

composite filaments and 5 wt% composites show optimum improvement in mechanical performance with an 18.1% and 16.8% increase in tensile strength and tensile modulus respectively compared to the neat PLA matrix. Similarly, an increase of 18.8% and 16.3% has been observed in the flexural strength and flexural modulus of elasticity respectively. Similarly, chitin and chitosan incorporated PLA composites prepared by FDM technique offer enhanced tensile strength, flexural strength and ductility over pristine PLA [42]. Composite added with 0.5 wt% chitin offers an increased density of 1.285 g/cm^3 and yields a tensile and flexural strength of 6.9 MPa and 10.4 MPa respectively. Ellessawy et.al developed eco-friendly filaments from recycled PET by incorporating date palm fibre nanopowder as a reinforcement agent by extrusion printing at 270°C with screw speed 70 rpm and heating power of 2 KW and the resultant composite, as shown in Fig. 3(a and b), is utilised for sustainable interior designs for furniture and fixtures [43]. The composite with a nanopowder content of 10% shows excellent values of tensile modulus of $846.7 \pm 20.8 \text{ MPa}$ and tensile strength of $49.4 \pm 3.6 \text{ MPa}$ respectively. The increased stiffness and good interfacial distribution between the matrix and filler exhibits the capacity to tolerate increased stress at the same strain area and increased Young's modulus. A porous lattice was reported from Tungston (W) alloy of $\text{W}_{93}\text{Ni}_{4.9}\text{Fe}_{2.1}$ mixed with PVA and glycerol by a material extrusion technique at a temperature from 150°C to 170°C , offering improved compressive resistance, ultimate compressive strength of 1442 MPa and

plastic strain of 19.8% for an extrusion temperature of 170°C , and exceptional formability with environmental [44]. The viscous flow activation energy of $1.64 \text{ kJ}\cdot\text{mol}^{-1}$ shows the smooth extrusion of slurry for the extrusion printing which also confirms the effectiveness of mechanical alloying.

2.2. Powder bed and ink-jet 3D printing

Powder bed fusion and ink-jet printing techniques utilise a laser beam to selectively fuse the layers of powder in a powder bed one by one. As shown in Fig. 2(b), this technology is based on powder processing, in which the spread powders on the build platform are selectively combined into a patterned layer by depositing a liquid binder through an inkjet printhead that can move in the X-Y direction. After the formation of the first layer, the platform will be lowered, and the next layer of powder will be spread. This process repeats, and final products will be formed. The final product from this AM technique is influenced by factors such as powder size, the viscosity of the binder, the interaction between the binder and powder, and the deposition speed. This AM technique has the advantage of room temperature processing and does not require any support structures.

Recently, 3D printed composites from microporous Silicon nitride (Si_3N_4) incorporated with polyamide (PA12), as shown in Figs. 3(c), 3 (D) printed (layer thickness $100 \mu\text{m}$, powder surface temperature 166°C ,

Table 1
Recent progress of eco-friendly materials-based polymer composites by 3D printing.

Composite Materials	AM Technique	Synthesis parameters	Recyclability	Application	Advantages	Ref
PLA/ ferronickel slag (FNS)	Material Extrusion	FNS (2.0, 4.0, 5.0, 6.0, 10.0, and 14.0 wt%) incorporated in PLA		Composite development	18.6%, 16.8%, 18.8% and 16.3% increments in the tensile strength, tensile modulus, flexural strength and flexural modulus	[41]
PLA/Chitin & chitosan	FDM			Food packaging	Improved density (1.285 g/cm ³) tensile (6.9 MPa), flexural strength (10.4 MPa) and ductility	[42]
Reinforced PET/ date palm frond nanoparticles	Material Extrusion	Extruded at 270 °C with screw speed 70 rpm and heating power of 2 KW	Recycled PET from drinking water bottle	Design and construction industries	Improved mechanical properties (tensile modulus of 846.7 ± 20.8 MPa and tensile strength of 49.4 ± 3.6 MPa)	[43]
PVA/glycerol/W ₉₃ Ni _{4,9} Fe _{2,1}	Material Extrusion	Extruded at a temperature of 150–170 °C		Environmental applications	Improved mechanical properties (ultimate compressive strength of 1442 MPa and plastic strain of 19.8%)	[44]
PA12/Si ₃ N ₄	Powder bed fusion	Layer thickness 100 µm, powder surface temperature 166°C, and laser speed 350–850 mms ⁻¹		High temperature applications	Improved mechanical and microstructure	[45]
Polyetheretherketone/ carbon fibre	Powder bed fusion	Post processing such as annealing and solvent induced crystallization		Industrial applications	Improved mechanical strength of 50 MPa	[46]
Polyamide 12/glass fibres	Powder bed fusion	Powder surface temperature 160°C, spreading velocity of 200 mms ⁻¹ print speed 180 mms ⁻¹		Boosting the performance	Enhancement in Young's modulus and flexural modulus of 54.3% and 36.7% and flame-retardant properties.	[47]
Polyurea/graphene	DLP	Layer thickness 0.05 mm. Post curing under UV (wavelength 390–410 nm, light intensity 40 cm ⁻²)	Recycling compatible	Nominal environmental impacts	superior mechanical properties (Young's modulus 39.9 MPa, impact strength of 64.6 KJ/m ² and an elongation at a break of 190.3%) and recyclability	[49]
ABS/Carbon black	DLP	Layer thickness 50 µm, UV light source (405 nm, intensity of 5 mW/cm ²)	Recycled carbon black	Solve the shrinkage issue	Improved hardness of 848 ± 0.6 and impact strength of 0.0790 ± 0.0143 mJm ⁻²	[48]
AESO-IBOMA/biochar	LCD	Layer thickness between 0.01 and 0.30 mm and a printing volume of 16.5 (l) × 7.2 (w) × 18 (h) cm ³		Biomedical sector	Improved storage modulus of 1315 MPa and Young's modulus of 679 MPa with cost-effective and ecofriendly products.	[50]
Polyamide 12/biochar	SLS	Layer thickness 0.175 mm, laser power multiplier to 1.0, and print surface temperature offset to -2.0 °C	Recycling compatible	Advanced sustainable 3D printing	Improved mechanical performance (tensile modulus, tensile strength, impact strength, flexural modulus and flexural strength are 3.2 GPa, 64.7 MPa, 3.0 kJ·m ⁻² , 1.5 GPa, and 100.9 MPa)	[51]
peanut husk powder/ polyether sulfone	SLS	Preheating temperature 82 °C, laser power 14 W, layer thickness 0.15 mm, 75 °C processing temperature, 2 m/s scan speed, and 0.2 mm scan spacing		Wooden flooring industry	Improved mechanical performance (tensile strength, impact strength, and bending strength as 1.1825 g/cm ³ , 6.076 MPa, 2.12 kJ/cm ² , 14.1 MPa respectively)	[52]
Polyamide 12/Lignin	SLS			Cost-effectiveness and improved processability	Improved stiffness (about 16%) and porosity (about 10%)	[53]
Poly (butylene adipate-co-terephthalate)/biofillers	SLS	Preheating temperature 63 °C, laser scan speed of 2400 mm/s for the infill region and 3840 mm/s for the border	Biofillers from agrowastes	Biomedical sector	Improved porosity about 63% and storage modulus of 224 MPa	[54]
Rosin/graphite/carbon black	DIW			Sustainable and green electronics	Excellent conductivity of 1500 S/m, and a sheet resistance of 7.82 Ω/sq	[57]
TEMPO Cellulose/graphene oxide	DIW			Biobased green conductive inks	Excellent shielding effectiveness of 55.6 dB and compression modulus of 250–1096 kPa	[58]
Conductive ink on the dielectric High-Tg substrate	Non-contact digital DIW			Eco-friendly PCB manufacturing	Reduced production cost	[59]
Cellulose nanocrystals/gelatine	DIW	Printing speed of 15 mms ⁻¹ , infill density 30%. diameter and height of the print 30 mm and 5 mm		Biomedical applications	High porosity and swelling ratio	[20]

and laser speed 350–850 mms⁻¹) by the powder bed fusion technique [45]. They demonstrated a hybrid manufacturing of powder bed fusion with polymer infiltration and pyrolysis to enhance the microstructure and mechanical performance, such as compressive strength. The composites with amorphous SiCN(O) suffered degradation, whereas composites containing crystalline silicon nitride of about 20–40 vol% show the best oxidation resistance properties. Powder bed fusion of carbon fibre-reinforced polyetherether ketone composites has been reported by

Tian et al., and they obtained optimal mechanical strength and proposed post-processing of the composites [46]. After post processing such as annealing and solvent induced crystallization, the Z-axis tensile strength reached 50 MPa, (62% higher than neat samples). Enhanced mechanical and flame-retardant properties were reported by incorporating layered double hydroxide (LDH) surface-modified glass fibres in polyamide 12 matrix by powder bed fusion technique (powder surface temperature 160°C, spreading velocity of 200 mms⁻¹ print speed 180 mms⁻¹) [47].

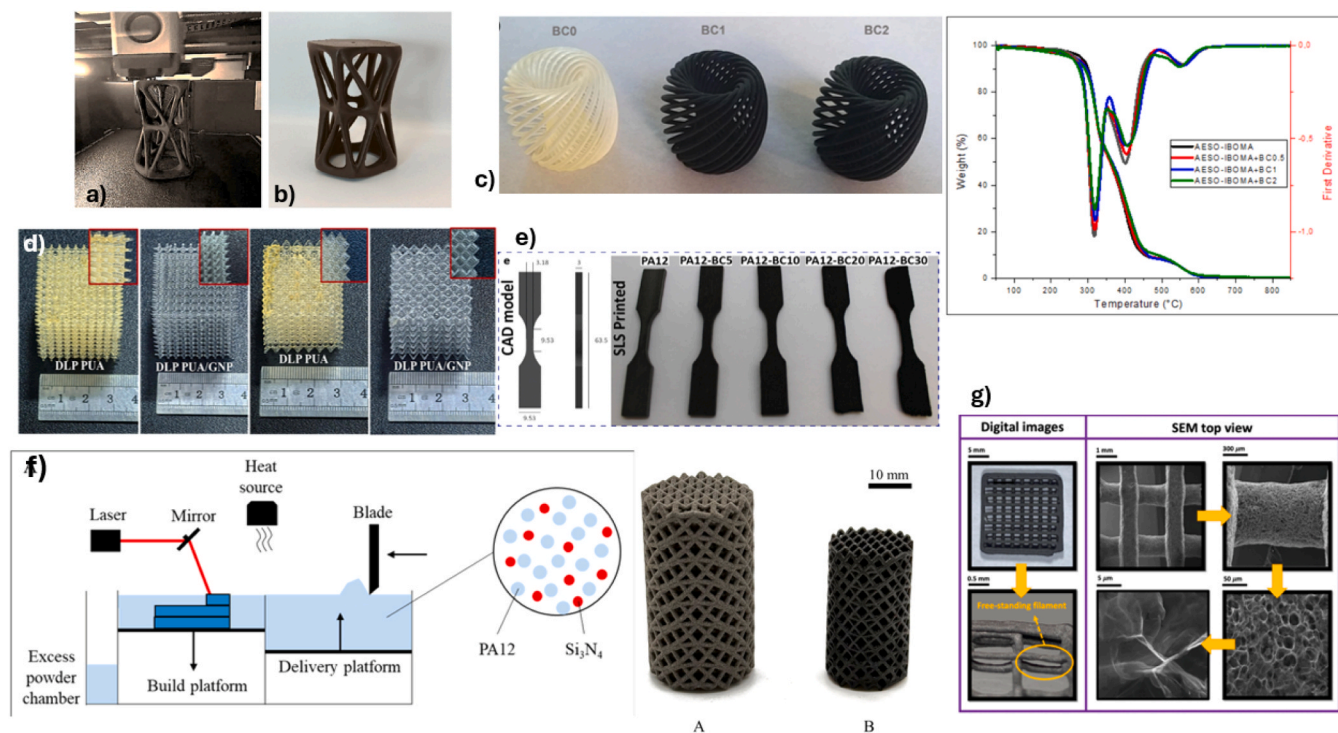


Fig. 3. Fabrication of 3D object design by various AM techniques; (a and b) PET/date palm fibre nanopowder composite by material extrusion.

They achieved enhancements in Young's modulus and flexural modulus of the printed composites by 54.3% and 36.7% respectively and proved the suitability of the powder bed fusion technique for manufacturing flame-retardant and high-performing composites. Compared with the peak heat release rate and total heat release of the composites, those of LDH modified glass fibers filled with polyamide composites were reduced by 17.7% and 12.7%, respectively. This work paves the way for PBF to prepare flame-retardant high-strength PA12 composites and provides a new solution to boost the performance of additively manufactured products.

2.3. Vat polymerisation

In the Vat polymerisation technique, a photosensitive liquid thermoset polymer experiences photolithographic cross-linking in a layer-by-layer manner to form a free-standing solid product. Stereolithography (SLA) is the primary technique in the vat polymerisation category, which utilises photopolymers that can be cured by a laser emitting in the UV range as the light source to induce layer-by-layer polymerisation and cross-linking of the liquid resin point by point. As shown in Fig. 2(c), a UV laser is directed along a desired path to irradiate the resin reservoir, and the photocurable resin polymerises into a 2D patterned layer. After each layer is cured, the platform lowers, and another layer of uncured resin is prepared for patterning. Typically, acrylic and epoxy resins are mainly used in SLA techniques. The primary advantage of SLA printing technology is its high-resolution printing, which prevents nozzle clogging due to its nozzle-free method. Digital light processing (DLP) is another technique in this category where each layer is being exposed at once, instead of point by point, to a selectively masked light source. Other techniques belonging to this category include continuous liquid interface production (CLIP), liquid crystal display (LCD), 3D printing, two-photon polymerisation (2PP), and multiphoton polymerisation (MPP).

Vat polymerisation-based AM technology has been widely employed to fabricate eco-friendly composites. Among these techniques, digital light processing (DLP) presents several major challenges, including

dimensional shrinkage defects and a lack of mechanical performance. Lin *et al.* recently developed a low-shrinkage composite using eco-friendly carbon black via the DLP technique (layer thickness 50 μm , UV light source (405 nm, intensity of 5 mW/cm^2) [48]. Out of the developed composites termed as sulfurized, de sulfurized and polyurethane-encapsulated carbon black, the latter one achieved a stress strain, impact strength, and hardness of 401.5/9.35%, 0.0790 \pm 0.0143 mJm^{-2} , 848 \pm 0.6 respectively for 1 h of UV curing. In another report, an eco-friendly, rapidly cured polyurea elastomer was 3D printed using the digital light processing (DLP) technique (layer thickness 0.05 mm and post curing under UV light of intensity 40 cm^{-2} at a wavelength 390–410 nm), achieving a tensile strength of 11.1 MPa, Young's modulus 39.9 MPa, change of impact strength of 64.6 KJ/m^2 and an elongation at a break of 190.3% [49]. They also investigated the incorporation of graphene nanoplatelets (GNPs) into the polyurea matrix through hydrogen bonding and lone pair- π stacking interactions between graphene and polyurea chains. The 3D-printed nanocomposites of polyurea/graphene, as shown in Fig. 3(d), exhibited a tensile strength of 7.3 MPa and an elongation at a break of 239.4%. The highest tensile strength of 12.9 MPa and elongation at a break of 399.2% has been achieved with 0.10 w.% graphene addition displays an increment of 76.7% and 66.8%, respectively, compared to neat DLP polyurea elastomer. The DLP polyurea elastomer exhibits recovered tensile strength and elongation at break of 2.7 MPa, 4.1 MPa, 5.2 MPa and 5.7 MPa, and 18.8%, 26.1%, 84.4% and 166.0%, respectively after healing of 5, 10, 15 and 20 h. Moreover, the elastomer achieves an excellent tensile strength healing efficiency (76.1%), elongation at break efficiency (166.0%) after curing at 120 $^\circ\text{C}$ for 20 h, tensile strength recovery (\sim 87.6%), and elongation at break recovery (203.3%) after dissolved in dimethyl formamide. The recycling and reprocessing of composite resins support a sustainable 3D printing approach, having excellent mechanical performance with minimal wastage. Colucci *et al.* recently reported a bio-based composite by adding biochar to the matrix of acrylate epoxidised soybean oil (AESO) and isobornyl methacrylate (IBOMA), as helical complex geometry which ensures the structural integrity as shown in Fig. 3(e), using a liquid crystal display (LCD) 3D printing technique

(layer thickness between 0.01 and 0.30 mm and a printing volume of $16.5 \text{ (l)} \times 7.2 \text{ (w)} \times 18 \text{ (h)} \text{ cm}^3$) [50]. The storage modulus value of composite with 1 wt% of biochar increases to 1315 MPa from 1140 MPa for the neat sample whereas the loss modulus increases with 0.5 wt% of biochar as 133 MPa from 117 MPa and decreases for 2 wt% biochar addition as 104 MPa. The Young's modulus also shows increased values from 634 MPa to 679 MPa for 1 wt% biochar added composites. This approach exhibits greater cost-effectiveness than other VAT polymerisation technologies and offers eco-friendly products with excellent resolution, printing speed, and enhanced mechanical properties.

2.4. Selective laser sintering (SLS)

The selective laser sintering (SLS) technique is based on powder processing, whereas inkjet 3D printing uses a laser beam instead of a liquid binder. In a typical SLS process, as shown in Fig. 2(d), a laser beam with a controlled path scans the powders, sinters them, and the powders fuse together through molecular diffusion. After sintering the first layer, processing of the next layer begins. The size of the powder particle, laser power, scan spacing, and speed are the main factors affecting the feature resolution of the final product. Among other AM techniques, SLS has the capability to create complex and high-resolution 3D-printed parts without the need for supportive materials.

A recent investigation employed biochar as a renewable filler in polyamide 12 (PA12) to fabricate composites, as shown in Fig. 3(f), by SLS printing (layer thickness 0.175 mm, laser power multiplier to 1.0, and print surface temperature offset to $-2.0 \text{ }^\circ\text{C}$) and exhibited an increment of tensile modulus and tensile strength from $1.4 \pm 0.1 \text{ GPa}$ to $3.2 \pm 0.3 \text{ GPa}$ and $43.1 \pm 1.2 \text{ MPa}$ to $64.7 \pm 2.0 \text{ MPa}$, respectively, for a 10 wt% of biochar [51]. Similarly, the impact strength, flexural modulus and flexural strength of 10 wt% of biochar incorporated PA12 composite shows an increment from 3.6 ± 0.2 – $3.0 \pm 0.1 \text{ kJ}\cdot\text{m}^{-2}$, 1.0 ± 0.0 – $1.5 \pm 0.1 \text{ GPa}$, and 65.2 ± 3.1 – $100.9 \pm 4.3 \text{ MPa}$ respectively. The elongation at break of composite is reduced from 12.1 ± 0.5 – $4.1 \pm 0.3\%$ with the biochar content due to the inherent brittleness of biochar. Moreover, biochar significantly lowers the carbon footprint by a 66% decrement in climate change potential from $11.53 \text{ kg CO}_2\text{-equiv}\cdot\text{kg}^{-1}$ for neat polyamide to $9.33 \text{ kg CO}_2\text{-equiv}\cdot\text{kg}^{-1}$ for 20 wt% biochar incorporated composites over 20 printing cycles. A sustainable composite of peanut husk powder/polyether sulfone has fabricated using the SLS technique (Preheating temperature $82 \text{ }^\circ\text{C}$, laser power 14 W, layer thickness 0.15 mm, $75 \text{ }^\circ\text{C}$ processing temperature, 2 m/s scan speed, and 0.2 mm scan spacing) [52]. Here, the SLS specimens had inner hole sizes of $\leq 0.125 \text{ mm}$ with peanut husk particles, which offer highest values of density, tensile strength, impact strength, and bending strength as $1.1825 \text{ g}\cdot\text{cm}^{-3}$, 6.076 MPa , $2.12 \text{ kJ}\cdot\text{cm}^{-2}$, 14.1 MPa respectively. Post processing with wax infiltration enhances density, tensile strength, impact strength, and bending strength to $2.0625 \text{ g}\cdot\text{cm}^{-3}$, 7.476 MPa , $2.96 \text{ kJ}\cdot\text{cm}^{-2}$, and 15.7 MPa respectively. Lignin has reported as a sustainable material for the SLS technique of producing composites with polyamide (PA12), which exhibits higher porosity of about 10% and increased stiffness in terms of by about 16% increment in Young's modulus and about 7% decrement in tensile strength [53]. Sustainable composites by incorporating agrowaste-derived biofillers into the poly (butylene adipate-co-terephthalate) matrix have developed by SLS printing (preheating temperature $63 \text{ }^\circ\text{C}$, laser scan speed of 2400 mm/s for the infill region and 3840 mm/s for the border) [54]. The printed composites with various agrowastes shows improved porosity from 52% (for neat matrix) to 56% and 58% by incorporating 5 and 10 wt% of maize-wastes filler, respectively and to 61% and 63% by incorporating wine production waste-based fillers. The storage modulus also enhanced from 153 MPa to 224 MPa for 5 wt% wine production waste-based fillers incorporated composites. This work proves poly (butylene adipate-co-terephthalate) as a matrix and composite can be an effective alternative to conventional polymers, in terms of sustainable and economic aspects.

2.5. Direct ink writing (DIW) or 3D plotting

Direct ink writing, also known as 3D plotting, is a layer-by-layer deposition of viscous material, often referred to as ink, from a syringe onto a stationary printing platform. Here, the syringe head moves in three dimensions during the extrusion process, as shown in Fig. 2(g). The quality of the final print depends on the viscosity of the ink and the printing speed. Hydrogels and viscous materials are primarily printed using this technique, and the temperature of the printing platform has controlled to maintain shape fidelity [55]. The physical stabilisation of each hydrogel-based deposited layer to withstand its own weight, and to improve its resolution from a more precise and controlled structure to the final structure [24]. This technique is primarily used to produce biobased scaffolds and objects for biomedical applications [56]. Printed scaffolds from cellulose nanocrystals (CNC) and gelatin, featuring a high porosity of approximately 65%, degradability, and a swelling ratio of approximately 390–590, by DIW technique (printing speed of $15 \text{ mm}\cdot\text{s}^{-1}$, infill density 30%, diameter and height of the print 30 mm and 5 mm) and post processing by freezing at $-25 \text{ }^\circ\text{C}$ [20]. Recently, Das et al. prepared a sustainable composite ink based on natural Rosin with graphite and carbon black using direct ink writing as an alternative to conventional conductive inks [57]. The resultant ink exhibits excellent conductivity, with a range of 500–1500 S/m, and a sheet resistance of 14–7.82 Ω /sq, towards sustainable and green printing as an environmentally benign alternative to traditional conductive inks in electronic applications. Biobased and electrically conductive hydrogel inks from TEMPO-oxidised cellulose nanofibrils and graphene oxide were synthesised, and 3D objects have made, as shown in Fig. 3(g), by the DIW technique, for electromagnetic interference shielding applications [58]. The printing fidelity, structural stability, and shape retention of the 3D objects depend on the cellulose-to-graphene loading ratio, which offers a high shielding effectiveness of 55.6 dB and compression modulus in the range of 250–1096 kPa. The fabrication of an eco-friendly printed circuit board (PCB) has been achieved by a non-contact digital DIW technique to accomplish the substantial reduction in the production costs [59].

3. Additive manufacturing of polymer composites by 4D printing

4D (four-dimensional) printing is an AM technique that combines 3D printing with smart materials, which can alter their shape and thereby their properties over time while exposed to diverse types of stimuli, including light [60–62], temperature [63–66], body temperature [65, 67], enzyme [68], pH [69], electricity [70], and magnetic fields [71,72]. Such alterations can be controlled and pre-designed by exploring the properties of polymers and their molecular structure to design smart materials. While 3D printing is employed to manufacture complex structures, 4D printing further simplifies the design and manufacturing process, offering improved quality and reliability with reduced material wastage, as the structures self-improve their characteristics over time. The development of 4D printing promises to address critical issues related to production costs and complexity, while also enabling the creation of new, tunable, and adaptive materials for various industrial and biological applications. Commonly used polymers for 4D printing include shape-memory polymers, self-healing polymers, hydrogels, and liquid crystal elastomers, and typical 4D-based AM techniques are fused deposition modelling (FDM), direct ink writing (DIW), stereolithography (SLA), and selective laser sintering (SLS). Out of these techniques, FDM (which uses thermoplastic-based polymers) and DIW (which uses hydrogels) are extrusion-based, whereas SLA (which uses light-curable materials) and SLS (which uses thermoplastic polymers) are laser-based. Table 2 details the recent progress of eco-friendly materials-based polymer composites by 4D printing.

Table 2
Recent progress of eco-friendly materials-based polymer composites by 4D printing.

Composite Materials	AM Technique	Synthesis parameters	Stimuli	Mechanical properties	Shape memory properties	Application	Ref
PLA-PBAT/Fe ₃ O ₄	FDM	Nozzle temperature 200 °C ± 10, Printing speed 300 mms ⁻¹ , Layer thickness 0.4 mm	Magnetic field	16% increase in UTS (35.89 MPa) and a 15% increase in toughness (1691.10 mJ)	Nearly 100% shape recovery	Sustainable material for contactless actuation.	[71]
PETG/Carbon black	FDM	Nozzle temperature 200 °C, Printing speed 300 mms ⁻¹ , Layer thickness 0.4 mm	Temperature	Improved strength of 42.69 MPa, toughness of 7499 J	Recovery rate of over 97%	Advanced applications	[74]
PBSe-co-PBIs	FDM	Extrusion speed 30 rpm, nozzle diameter 0.4 mm	UV irradiation	Tensile strength and fracture strain of 29.3±2.3 MPa, 2079 ±345% and 19.5±2.6 MPa, 622±77% respectively for longitudinal and transverse to the printing directions	Excellent shape memory performance	High-temperature protection devices	[67]
TPU/multiwall CNTs	FDM	Nozzle temperature 260 °C, nozzle diameter 0.4 mm, print speed 30 mms ⁻¹ layer height 0.2 mm	Body temperature	Tensile strength of 26.5 ±0.4 MPa, elongation of 209.9 ±7, and hardness of 94	Shape-memory properties at body temperature of 37°C	Body sensing applications	[68]
PLA/APHA/TPU	FDM	Nozzle temperature 200–220 °C, Printing speed 300 mms ⁻¹ , Layer thickness 0.3–0.5 mm	Thermal & mechanical	Improved tensile strength (28.79 ± 0.16 MPa), elongation at break (521.26%), modulus (840.17 MPa), flexural strength (30.95 MPa), flexural modulus (1088.93 MPa)	Shape recovery at ~39.5°C, with near-complete shape fixity (~100%) and high recovery ratios (>92%)	Next-generation biomedical	[75]
NW-MO-TTMP/ethyl cellulose	DIW	Printing speed 7 mms ⁻¹ , print height 0.48 mm	UV light	Tensile strength of 20.6 MPa	Shape fixity ratio of 99.7% and shape recovery ratio of 98.6%	High-performance	[60]
PU/lignin nanotubes	DIW	Printing speed 150 mm/min, syringe pump injection rate 40 µL/min	UV light	Tensile strength of 16.4 MPa, fracture energy of 36.52 J/mm ²	Shape recovery rate of 99%	Smart biomaterials	[61]
AESO/polydopamine modified HAP	DIW	UV-DIW technology at 0 °C.	UV light		Shape memory performance of 97% in 16 s	Bone scaffold	[62]
poly (d,l-lactide-co-trimethylene carbonate) (PLMC)	DIW		Body temperature		Shape changing small structures with fast response	Biomedical devices	[69]
Methacrylated bovine serum albumin (MA-BSA)	DIW		Temperature/pH/enzyme	Compressive strength and compressive modulus of 2 MPa and 1.82 MPa (Temp-ink), 4.71 MPa and 2.16 MPa (pH-ink), and 0.11 MPa and 0.09 MPa (Enz-ink) respectively		Autonomous shape transformations	[76]
IBOMA-reinforced micro cellulose	SLA	Layer height 25 µm, lift speed 40 mm/min, retract speed 60 mm/min	Temperature	Young's modulus of 1.01 GPa, hardness of 72.3, ultimate tensile strength of 21 MPa, and strain at break of 8%	Shape fixity of > 99.5% and a shape recovery of > 95%	Mechanically competitive applications	[64]
PCL-Itaconic acid	DLP	Layer thickness 50 µm, light intensity 22 cm ⁻² with 22 s irradiation time	pH	Young's modulus of 33 MPa and an elongation at break of 52%		Biomedical devices	[77]
Acylated epoxidized soybean oil (AESO)	SLA	Printing speed of 60, 80, and 100 mms ⁻¹ , laser power 15 mW with frequencies of 140, 160, and 180 pulses/s. UV laser wavelength 405 nm	Temperature		Shape fixity of about 85% with a recovery time 1.6 s	Biomedical Engineering	[65]
RO-IBOA-IBOMA/carbon nanotubes	SLA	Layer height 50 µm and a layer time of 20 s, 60 s and 90 s for neat PCL and composites respectively	Light and temperature	Mechanical performance from 2.3 to 12.5 MPa	Shape fixity and shape recovery ratios up to 99%	Sustainable applications	[78]
TPAE	SLS	Sintering temperature 156 °C, laser power 21 W, layer thickness 0.10 mm and scan spacing 0.10 mm	Temperature	Tensile strength of 13.7 MPa, elastic modulus of 124 MPa and elongation at break of 200%)	Shape fixity of 76% and shape-recovery ratio of 89%	Soft robotics	[79]
TPAE	SLS		Temperature		Two-way shape memory effect	Temperature sensors	[66]
PUDA/carbon nanotube	SLS	Layer thickness 0.15 mm, laser power 60 W, and laser scan speed 7.6 ms ⁻¹	NIR		NIR-triggered self-healing and shape memory functions	Smart materials	[80]

(continued on next page)

Table 2 (continued)

Composite Materials	AM Technique	Synthesis parameters	Stimuli	Mechanical properties	Shape memory properties	Application	Ref
TPU/carbon nanotube	SLS	Laser scan speed 2000 mms^{-1} , hatching distance 0.1 mm and a layer thickness 0.12 mm	Heat and electric current	Elastic modulus of 43.30 GPa, ultimate tensile strength of 3.94 MPa, and elongation at break of 46.79%	Fast shape recovery of 25 s	High-tech applications	[70]
TPU-PLLA/ Fe_3O_4	SLS	Nozzle temperature 200 °C, Printing speed 300 mms^{-1} , Layer thickness 0.4 mm	Water and Magnetic field	Tensile strength of 9.24 MPa and hardness of 5.75 Hv	Shape recovery ratio of 95.92% and shape fixity ratio of 98.33% in 50 °C water, and a shape recovery of 73.14% under the alternating magnetic field	Bone tissue engineering	[72]

3.1. Fused deposition modelling (FDM)

FDM is the most used 4D printing technique, offering high-speed printing; however, the processing time is prolonged due to the use of polymer filaments. Additionally, preheating the polymer filament materials may limit temperature sensitivity and generate toxic vapours [73]. To improve the lower thermal stability and low melt flow index, Baghani et al. have blended PLA with poly (butylene adipate-co-terephthalate) (PBAT) and magnetic Fe_3O_4 nanoparticles using FDM 3D printing (nozzle temperature 200 °C, printing speed 300 mms^{-1} , and layer thickness of 0.4 mm) [71]. The resultant composite exhibits improved thermal stability and toughness, along with an excellent shape memory response, as shown in Fig. 4(a). With 10 wt% Fe_3O_4 incorporated composite achieved an ultimate tensile strength of 35.89 MPa, elongation of 7.55% and toughness of 1691.10 mJ to the UTS point and 6281.70 mJ to 30% elongation, showing an increment of 16% and 1.1%, 15% and 13%, respectively, with respect to neat polymer blend. All samples reveal nearly 100% shape recovery effect by using a high-frequency induction with a magnetic induction coil, but the recovery time varies depending on the amount of Fe_3O_4 nanoparticles in the composites. 10 wt% Fe_3O_4 incorporated composite starts to recover in 44 s and takes 64 s to fully recover. Similarly, composites with 15 wt % and 20 wt% Fe_3O_4 start to recover in 40 s and takes 54, and 56 s to fully recover. Poly(ethylene terephthalate) glycol (PETG) composites incorporating carbon black have been printed in 4D using the FDM process (nozzle temperature 200 °C, printing speed 300 mms^{-1} , and layer thickness 0.4 mm), exhibiting improved strength of 42.69 MPa (which has an increment of 14.8% compared to neat matrix), toughness of 7499 J to its stress level, and shape memory properties with an excellent recovery rate of over 97% [74]. The improvement in shape recovery, as shown in Fig. 4(b), is attributed to the formation of a physical network in the composite through the introduction of carbon black, which provides additional entropic elasticity that facilitates specimen restoration during the shape memory test, resulting in more effective shape recovery. Wu et al. developed biobased shape memory copolyesters (PBSe-co-PBIs) by polycondensation of dimethyl itaconate, dimethyl sebacate, and 1,4-butanediol using FDM-based UV assisted 4D printing (extrusion speed 30 rpm and nozzle diameter 0.4 mm) for high-temperature protection devices [67]. The resultant UV printed PBSe-co-PBIs exhibits tensile strength and fracture strain of 29.3 ± 2.3 MPa, $2079 \pm 345\%$ and 19.5 ± 2.6 MPa, $622 \pm 77\%$ respectively for longitudinal and transverse to the printing directions. Biobased and environmentally friendly conductive filaments have developed using the FDM technique (nozzle temperature 260 °C, nozzle diameter 0.4 mm, print speed 30 mms^{-1} and layer height 0.2 mm) with thermoplastic polyurethane (TPU) and multiwall carbon nanotubes. The resultant composite of TPU-MWCNT-3.25 exhibits excellent mechanical properties (tensile strength of 26.5 ± 0.4 MPa, elongation of 209.9 ± 7 , and hardness of 94) and a shape-memory property at body temperature (37 °C), primarily for body sensing applications [68]. A polymer blend filament composed of polylactic acid (PLA), amorphous

polyhydroxyalkanoates (APHA), and thermoplastic polyurethane (TPU) (PLA-APHA-TPU) has been 4D printed (nozzle temperature between 200–220 °C, printing speed 300 mms^{-1} , and layer thickness 0.3–0.5 mm) which enables a rapid shape recovery at $\sim 39.5^\circ\text{C}$, with near-complete shape fixity ($\sim 100\%$) and high recovery ratios ($>92\%$) for a PLA-APHA-TPU: 60–20–20 wt% composite, as shown in Fig. 4(c), under both thermal and mechanical stimuli [75]. Such dual stimulus responses have attributed to the synergy between ductile behaviour (arising from TPU) and flexibility and thermal sensitivity (arising from APHA). The printed composite of PLA-APHA-TPU: 60–20–20 wt% exhibits superior mechanical performance in terms of tensile strength (28.79 ± 0.16 MPa), elongation at break (521.26%), modulus (840.17 MPa), flexural strength (30.95 MPa), flexural modulus (1088.93 MPa).

3.2. Direct ink writing (DIW)

DIW is another extrusion-type AM technique which employs the extrusion of hydrogel or ink through a syringe. Here, the viscoelastic properties of the ink determine the printability and quality of the final structure, and thermal or photopolymerization-based post-processing steps have been used to solidify the inks, which play a key role in the 4D printing process. To improve the viscosity and printability of a shape memory polymer hydrogel derived from magnolol and trimethylolpropane tris(3-mercaptopropionate) (NW-MO-TTMP), biomass-derived ethyl cellulose has incorporated, and the material was 4D printed using the DIW technique [60]. Here, the printhead with a UV lamp (intensity ranging between 6–24 mW/cm^2) offers a print height of 0.48 mm by using 0.6 mm of nozzle diameter for a printing speed of 7 mms^{-1} . The resulting composite exhibits a tensile strength of 20.6 MPa compared to 2.7 MPa for neat NW-MO-TTMP, an excellent shape fixity ratio of 99.7%, and shape recovery ratio of 98.6%. Wang et al. developed shape memory polyurethane (PU) composites filled with lignin nanotubes by molecular assembly via DIW printing as UV-responsive shape recovery effect for smart biomaterials applications [61]. The DIW printing has performed at a printing speed of 150 mm/min with syringe pump injection rate of 40 $\mu\text{L}/\text{min}$. As shown in Fig. 5(a), the composites exhibit a shape recovery rate of 99% under UV radiation at 370 nm for 15 min, along with an excellent tensile strength of approximately 16.4 MPa (131% higher value compared to neat PU which is 7.11 MPa) and maximum fracture energy of 36.52 J/mm^2 . The specific mechanism and schematic illustration of dipole-dipole interactions (hydrogen bonding) between polyurethane and lignin nanotubes are shown in Fig. 5(d and e) respectively. Plant-based bone scaffolds have been developed by incorporating polydopamine-modified hydroxyapatite particles into acrylated epoxidised soybean oil (AESO) resin using UV-assisted DIW technology at 0 °C [62]. The resultant bone scaffolds displayed an optimum shape memory (97% in 16 s) and achieved 40 C within 4 min under 1 W/cm^2 NIR irradiation with outstanding osteogenic activity and met the mechanical requirements for a bone scaffold. A biocompatible poly (D,L-lactide-co-trimethylene carbonate) (PLMC) is

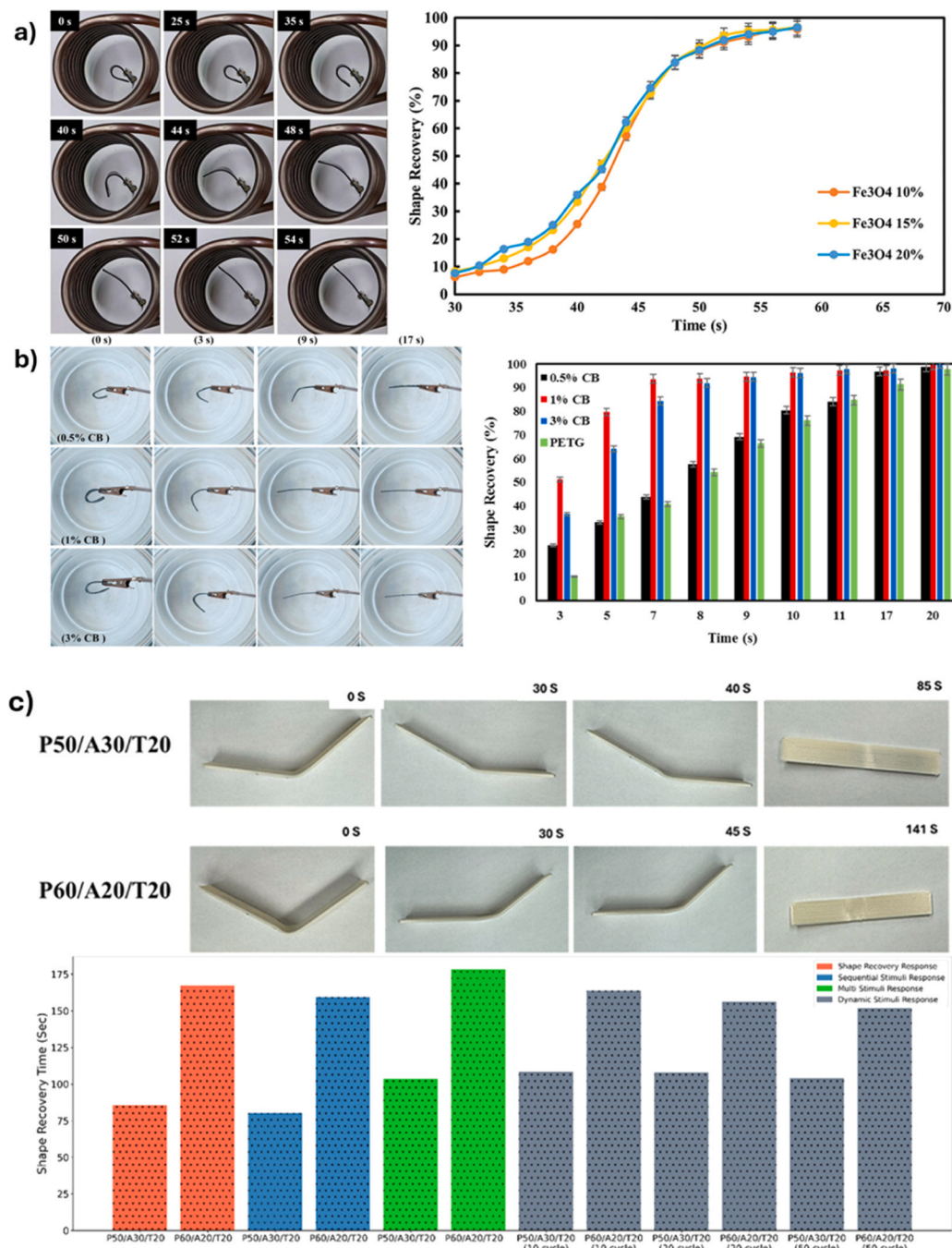


Fig. 4. (a) Shape recovery analysis of PLA-PBAT composite in a magnetic field for Fe₃O₄–20% (left) and the temporal evolution of shape recovery (%) in a magnetic field with respect to time (right)[71]. (b) Shape recovery process for PETG-Carbon black composites at different time intervals (left) and their shape recovery ratio over time [74]. (c) Shape memory behaviour of PLA/APHA/TPU blend generated by force and heat (top) and their shape recovery time under various stimuli (bottom)[75].

employed to develop shape-changing small structures with fast response around body temperatures as a potential candidate in the field of biomedical applications such as nonwoven fabric (3 s), surgical suture (4 s), and self-expandable stent (35 s) [69]. Protein-derived (methacrylated bovine serum albumin (MA–BSA)) hydrogels were developed as a multi-stimuli (temperature, pH, and enzyme) responsive material for DIW printing of multi-layered stimuli-responsive hydrogels [76]. The hydrogels based on temperature-ink, pH-ink, and enzyme-ink exhibit a compressive strength and compressive modulus of 2 MPa and 1.82 MPa, 4.71 MPa and 2.16 MPa, and 0.11 MPa and 0.09 MPa respectively. This approach offers shape transformations in response to changes in

atmospheric temperature, enzymatic degradation, and pH, demonstrating the capabilities of 4D printed methods.

3.3. Stereolithography (SLA)

Stereolithography (SLA) is a laser-based AM technique, which uses a laser light beam to photo-polymerise and cross-link photo-curable monomers for 4D printing. Digital light processing (DLP) also belongs to this category of printing, where it can solidify an entire layer of monomer at a time. DLP offers faster printing and production speed, but a lower resolution compared to SLA. Dicks et al. employed 4D printing via

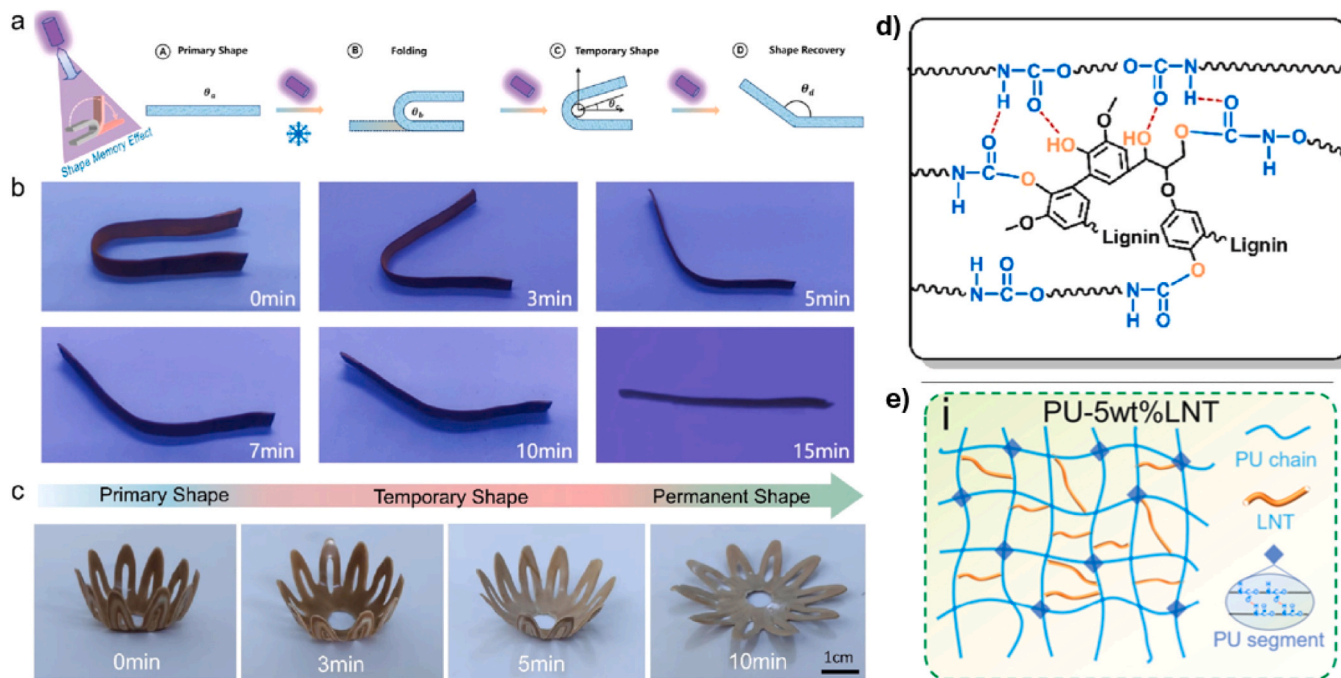


Fig. 5. (a) Schematic of the shape memory test, (b) digital photo of the shape memory recovery test, and (c) shape recovery process under different UV irradiation times, (d) mechanism diagram and (e) schematic diagram of the interaction between PU-lignin nanotube composites by DIW technique.

stereolithography (layer height $25\ \mu\text{m}$, lift speed $40\ \text{mm}/\text{min}$, and retract speed $60\ \text{mm}/\text{min}$) of itaconated castor oil monomer and isobornyl (meth)acrylate (IBOMA) reinforced with microcrystalline cellulose composites without compromising their mechanical performance and shape memory properties, as displayed in Fig. 6(A), with shape memory actuation at around 100°C [64]. IBOA-cellulose and IBOMA-cellulose composites show a Young's modulus of $0.86\ \text{GPa}$ and $1.01\ \text{GPa}$, hardness of 64.8 and 72.3 , ultimate tensile strength of $14.8\ \text{MPa}$ and $21\ \text{MPa}$, and strain at break of 8% , respectively. The resultant composites achieved a shape fixity of $> 99.5\%$ and a shape recovery of $> 95\%$. Heise et al. recently introduced a solvent-free approach by using polycaprolactone (PCL) and itaconic acid (IA) derived from biomass by pH-triggered 4D printing (layer thickness $50\ \mu\text{m}$, light intensity $22\ \text{mW}/\text{cm}^2$ with $22\ \text{s}$ irradiation time) shape transformations [77]. As shown in Fig. 6(B), the hydrogel exhibited a maximum degree of swelling at a pH of 10 due to the presence of IA units, which introduce cross-link points through their double bonds. The mechanical properties of PCL-IA networks show a Young's modulus of $33\ \text{MPa}$ and an elongation at break of 52% with respect to cross-link density decreases. A plant-based shape-memory polymer derived from acrylated epoxidised soybean oil (AESO) has been 4D printed by SLA (printing speed $60, 80,$ and $100\ \text{mms}^{-1}$, laser power $15\ \text{mW}$ with frequencies of $140, 160,$ and $180\ \text{pulses}/\text{s}$) to develop biomedical engineering devices [65]. They achieved a maximum fixity of approximately 85% with a lower recovery time of $1.6\ \text{s}$ with a UV laser wavelength of $405\ \text{nm}$. Recently, a fully biodegradable shape memory polymer matrix from rapeseed oil (RO), isobornyl acrylate (IBOA), and isobornyl methacrylate (IBOMA) has been developed by incorporating carbon nanotubes via 4D printing with a layer height $50\ \mu\text{m}$ and a layer time of $20\ \text{s}, 60\ \text{s}$ and $90\ \text{s}$ for neat PCL and composites respectively [78]. The resultant composites exhibited excellent shape fixity and shape recovery ratios up to 99% , as shown in Fig. 6(C), with an outstanding mechanical performance ranging from 2.3 to $12.5\ \text{MPa}$.

3.4. Selective laser sintering (SLS)

SLS is a powder-based AM technique which uses a laser beam to heat

powders and converts them to a semi-liquid state in a pre-designed layered structure. The processing speed of SLS is usually faster than FDM and SLA because it does not require scaffold structural support. Polymers such as thermoplastic polyurethane (TPU), polyamide (PA), and PDMS are employed for 4D printing by the SLS technique. Recently, thermoplastic polyamide elastomer (TPAE) has been 4D printed by the SLS technique (sintering temperature 156°C , laser power $21\ \text{W}$, layer thickness $0.10\ \text{mm}$ and scan spacing $0.10\ \text{mm}$) with excellent mechanical properties (tensile strength of $13.7\ \text{MPa}$, elastic modulus of $124\ \text{MPa}$, and elongation at break of 200%) [79]. As shown in Fig. 7, the composites exhibit average shape-fixing ratios and shape-recovery ratios of 76% and 89% , respectively, for a strain programming of 10% and 15% , demonstrating excellent and stable shape memory behaviour. In another report, a series of TPAsEs have been printed by SLS through the polycondensation reaction of PA1212 prepolymer and polyetheramine, which exhibits a reversible two-way shape memory effect [66]. Xia et al. developed composites based on polyurethane with a reversible Diels-Alder bond (PUDA) incorporated with carbon nanotubes by SLS 4D printing (layer thickness $0.15\ \text{mm}$, laser power $60\ \text{W}$, and laser scan speed $7.6\ \text{ms}^{-1}$) [80]. The composites stimulated by NIR exhibit self-healing and shape-memory properties. Recently, thermoplastic polyurethane (TPU) filled with carbonaceous particles, such as carbon fibres and carbon nanotubes, have been fabricated by SLS technique (laser scan speed $2000\ \text{mms}^{-1}$, hatching distance $0.1\ \text{mm}$ and a layer thickness $0.12\ \text{mm}$) [70]. The SLS printed TPU composite with $20\ \text{wt}\%$ of hybrid filler exhibits an elastic modulus of $43.30 \pm 3.14\ \text{GPa}$, ultimate tensile strength of $3.94 \pm 0.01\ \text{MPa}$, and elongation at break of $46.79 \pm 3.29\%$ and the composite has a fast shape recovery of $25\ \text{s}$. The resultant nanocomposites have triggered by heat and electricity, in which the shape recovery process has shown to be almost four times faster when triggered by electric currents than when triggered by direct heating, with a higher shape recovery ratio. TPU, which combines poly(L-lactic acid) (PLLA), reports excellent biocompatibility and shape memory abilities by incorporating Fe_3O_4 nanoparticles through SLS 4D printing (nozzle temperature 200°C , printing speed $300\ \text{mms}^{-1}$, and layer thickness $0.4\ \text{mm}$) [72]. The resultant $10\ \text{wt}\%$ Fe_3O_4 composite exhibits an increment in tensile strength and hardness from 8.43 to

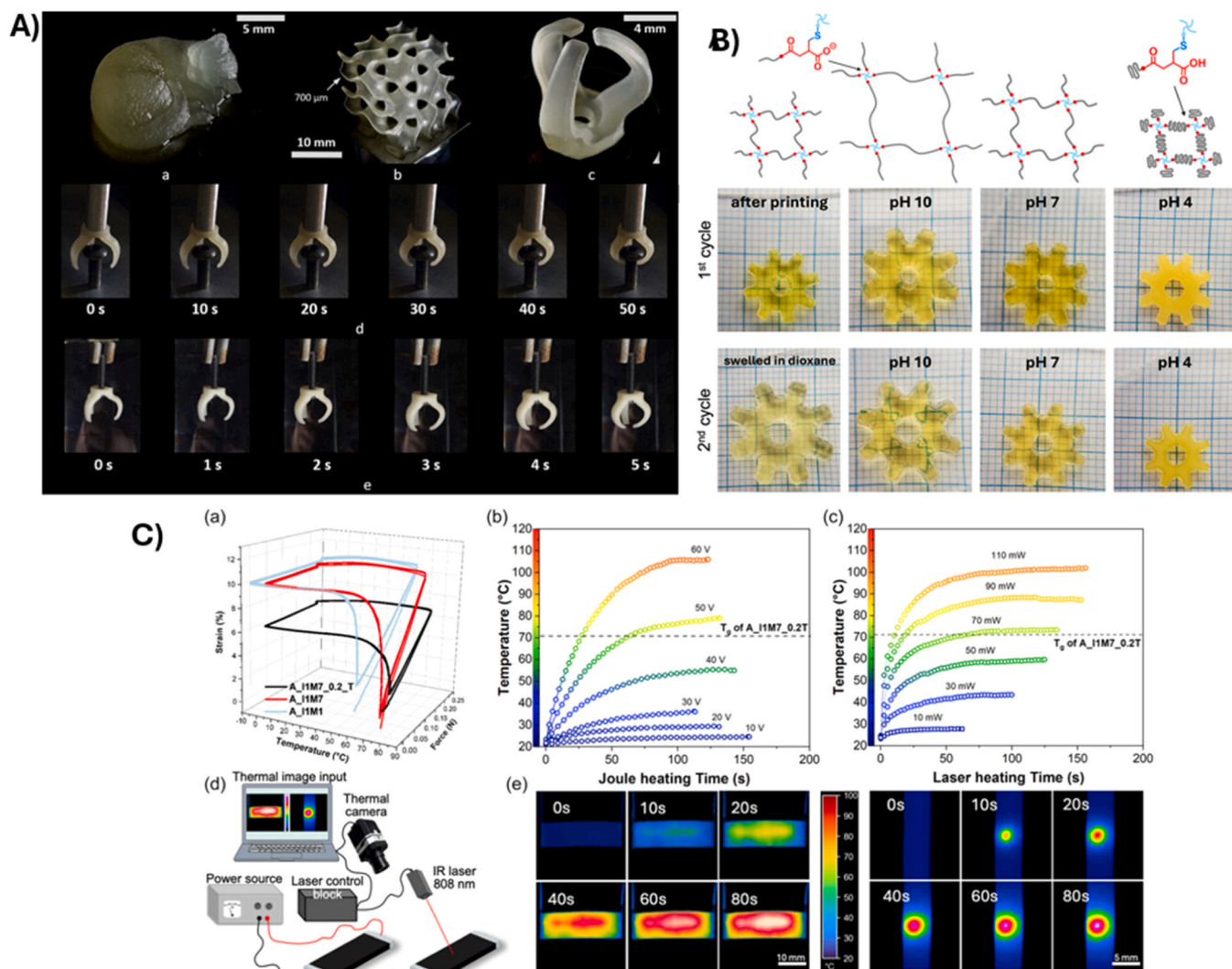


Fig. 6. (a) 3D scanned sleeping cat, (b) organoid structure, (c) robotic gripper of SLA printed objects of IBOA-reinforced micro cellulose particles, (d) shape recovery using hot air for actuation, and (e) shape recovery using near-boiling water (A) [64]. Schematic illustration of the network swelling as a function of pH and digital images of the DLP printed structure of PCL-IA swelled in different buffer solutions for two cycles (swelling time 24 h) (B) [77]. (a) Shape memory cycles indicating shape recovery and fixation, (b) maximum temperature variations during Joule heating at increasing applied voltages. (c) maximum temperature variations during light irradiation under increasing laser power (808 nm), (d) experimental setup for thermal imaging, (e) thermal images of heating by electricity (left, 60 V) and light (right, 110 mW) (C) [78].

9.24 MPa and 4.41–5.75 Hv compared with the neat polymer blend. The 10 wt% Fe₃O₄ composite exhibit excellent shape recovery ratios in 50 °C water, increasing from 66.67% to 95.92%, and shape fixity ratio of 98.33% while under the alternating magnetic field, it has a shape recovery of 73.14% demonstrating outstanding biocompatibility.

4. Sustainability and environmental aspects of additively manufactured polymer composites

Sustainability awareness in product design and manufacturing has grown significantly, focusing on factors such as resource efficiency, pollution, safety risks to humans and ecosystems, product durability and performance, and overall life cycle costs. Within this broader context, AM is often promoted as a tool to support more sustainable and circular production, but the extent to which AM of polymer composites delivers net benefits is strongly context dependent [81]. The key idea of sustainability in the AM of polymer composites includes the use of eco-friendly reagents and feedstocks from renewable and biodegradable resources, the possibility to design lightweight and highly optimised structures, and in some cases the capability to reprocess materials to

support circular economy strategies. To evaluate these claims, it is essential to assess actual net waste reduction, energy demand and associated costs in comparison with traditional manufacturing methods. Generally, AM is considered environmentally promising where it can enable localised or on demand production, reduce overproduction and tooling needs, and thus reduce geometric material waste and transportation-related emissions by eliminating the need to ship finished products from centralised factories. Additionally, AM enables material savings through lightweight design of components, achieved via topology optimisation and lattice structures. However, these potential advantages only translate into lower life cycle impacts when the additional energy use, process complexity and end of life implications of AM and its feedstocks are properly accounted for [82].

Compared to conventional methods, AM can offer environmental advantages such as reduced geometry related material waste, better buy-to-fly ratios, and the possibility of localised production that may decrease transportation related emissions. In the biomedical field, the use of biocompatible materials and patient specific designs offers potential sustainability benefits through reduced excess material usage while maintaining high accuracy and producing customised products

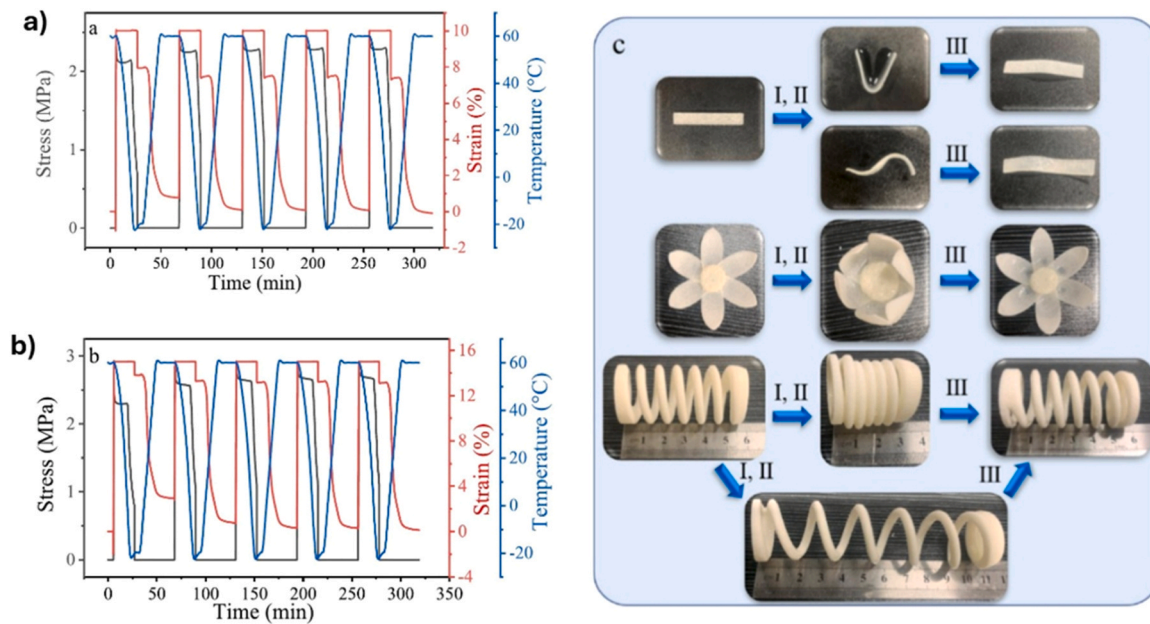


Fig. 7. DMA characterisation for (a) 10% strain, (b) 15% strain, and shape memory behaviours of SLS printed thermoplastic polyamide elastomer (TPAE) parts (c) (I: Deforming at 60 °C with external force for 0.5 h; II: Cooling down to -20 °C and removing the external force; III: Heating to 60 °C).

that closely match human anatomy. Choudhary et al. developed a sustainability assessment framework for a biomedical scaffold from a life cycle perspective, evaluating economic, environmental, and social aspects by comparing fabrication via additive (AM) and traditional (TM) manufacturing routes. In their specific case study on a PLA/alumina scaffold produced by FDM and freeze drying, the AM route showed approximately 20% lower cost and a much higher composite sustainability index (0.9271 for AM vs 0.0136 for TM), mainly due to environmental and social indicators as shown in Fig. 8 [83].

Despite the growing use of AM, there is a significant lack of focus on its sustainability and broader environmental implications, highlighting the need for a more comprehensive evaluation of its overall impact. Soares et al. applied the S-LCA framework to compare medical devices fabricated using ABS by fused filament deposition with a conventional method and proved that AM supports social sustainability by contributing positively to the creation of specialised local employment and promoting broader technological and economic advancement [84]. However, AM is not without its environmental costs, as it still relies on energy and material consumption and can emit pollutants. Assessing the

environmental implications of AM is challenging and complex, due to the broad and growing array of variables influencing AM, including material types, feedstock forms, manufacturing processes, geographic factors, and post-processing methods [85]. Energy use remains a major concern, with process efficiency varying based on feedstock, technology, usage patterns, and location. Health risks have also been identified, particularly in relation to machine operation and the release of airborne particles and volatile organic compounds. Waste generation during AM remains another concern [85]. Increasing attention is being directed toward developing polymer composites reinforced with bio-based materials, as these are recognised as environmentally friendly and sourced from naturally occurring resources. Such bio-reinforcements are incorporated into polymer matrices to enhance the performance of composites. In this context, utilising bio-based and fibre-reinforced materials is gaining traction as a potentially more sustainable alternative, although their actual life-cycle performance remains dependent on cultivation, processing, durability in use and end-of-life options.

AM could potentially perform better in terms of environmental impact when one or more of the following conditions are met: (i) parts are highly complex or strongly customised, (ii) topology optimisation and part consolidation significantly reduce mass and number of components, (iii) utilisation rates of AM equipment are high, (iv) low carbon electricity is available, and (v) effective closed loop or high value recycling of polymer/fibre feedstocks is implemented. When AM is used to reproduce simple parts without design changes, with low machine utilisation, in carbon intensive grids, and without robust recycling, it can result in high energy use and climate impacts.

5. Recycling aspects of additively manufactured polymer composites

As plastic waste pollution remains a pressing global issue, research efforts have intensified in creating bio-based substitutes for conventional petroleum-based plastics and improving biodegradation and recycling strategies. One promising strategy involves utilising recovered and repurposed materials as feedstock in AM processes. Transforming plastic waste into filaments suitable for 3D printing provides access to a diverse range of materials [86]. However, recycling of polymer composites remains particularly challenging in such a way that such

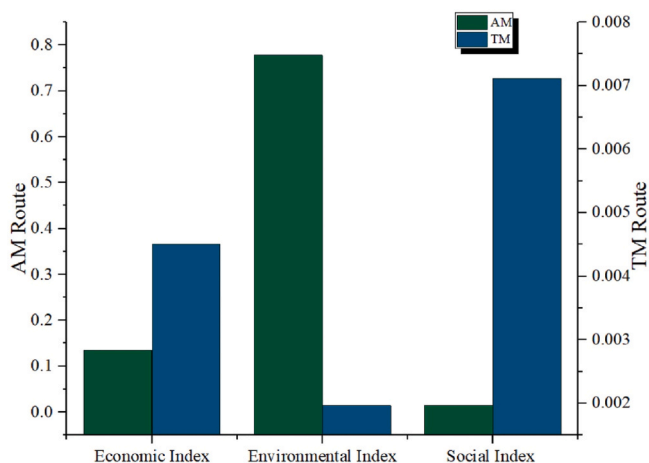


Fig. 8. Sustainability index for additive manufacturing (AM) and traditional manufacturing (TM) network routes.

composites often include fibres or fillers, which complicate conventional recycling processes and result in low recycling rates, typically around 5% [87]. Furthermore, the quality of recycled polymers tends to deteriorate with each reuse cycle, making them less suitable for demanding applications [88].

The recycling of polymeric material for AM typically involves several stages, such as sorting, cleaning, decontamination, grinding, remelting, and extrusion [86]. During the collection, plastic waste is collected directly at the source and handling recycling locally has proven to be more efficient and easier to manage than centralised methods. During sorting, accounting for approximately a quarter of the recycling process, the collected plastics are classified into distinct categories based on their properties. The approach to recycling varies depending on the specific polymer type, and the separation of mixed polymers presents a substantial challenge due to the difficulty of distinguishing them [89]. During cleaning, impurities such as labels and adhesives attached to the waste are eliminated. Following this, the shredding process breaks down defective prints and other plastic residues into smaller fragments, resulting in easier handling and processing due to increased surface area. The shredded plastics are then converted into a usable form, such as pellets. Plastic recycling methods are generally grouped into three main types: (i) mechanical, (ii) chemical, and (iii) thermal recycling.

Mechanical recycling involves recovering and transforming polymer materials into new products using methods that reshape plastic waste without changing its chemical composition. This approach uses size reduction, sorting, cleaning, remelting, and product manufacturing techniques. The process of mechanical recycling is associated with energy use and environmental benefits, particularly for waste streams from plastic or bioplastics [86,90]. Chemical recycling is more complex and expensive, requiring greater labour and energy inputs and potentially generating additional pollutants. Nonetheless, it can substantially reduce overall energy use.

To establish the circular economic potential through AM processes, Peeters et al. employ an interpretive structural modelling (ISM) method to refine the structural relationships among the barriers to distributed recycling of 3D printing waste to promote sustainability [91]. A recent study examined the utilisation of PET waste derived from plastic bottles in a custom-made filament extrusion setup for 3D printing applications. Waste PET bottles were cut into strips and then processed into filaments using a modified volcano nozzle. The method successfully produced recycled polyethylene terephthalate (rPET) and rPET/PA6-CF composite filaments, confirming their compatibility with the fused filament fabrication (FFF) process. Mechanical testing revealed that rPET/PA6-CF composites demonstrated enhanced tensile strength compared to pure

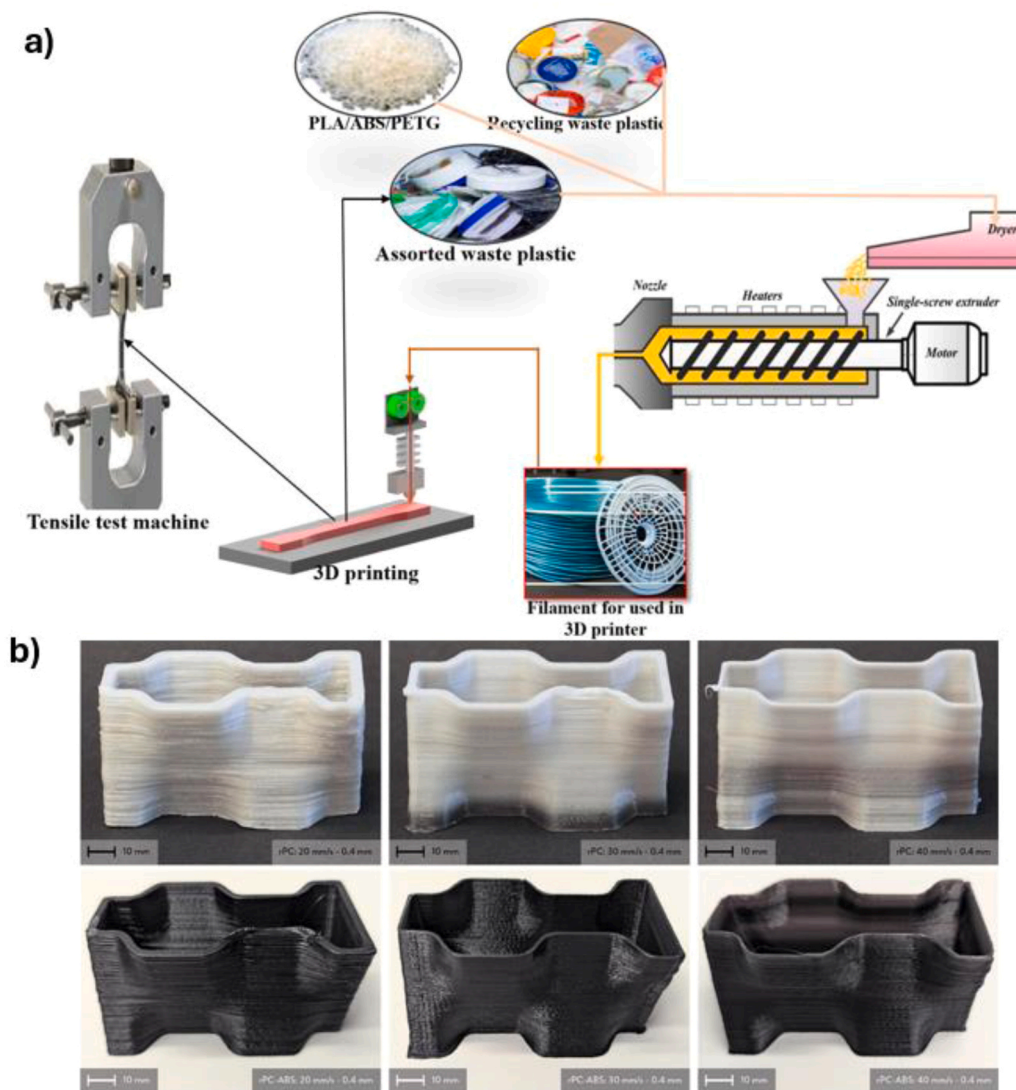


Fig. 9. (a) Schematic of the recycling process of PLA-ABS-PETG and formation of filaments from recycled plastic waste for 3D printing [88]. (b) Distributed recycling 3D printed samples from recycled polycarbonate (PC) (top) and recycled PC/ABS (bottom).

rPET, highlighting the strengthening effect provided by carbon fibres. Nevertheless, the composites showed a slight decrease in failure strain and Young's modulus, indicating a compromise between mechanical strength and flexibility [[89]. Better printability and the fabrication of

complex patterns, as shown in Fig. 9, were achieved with the distributed 3D printing technique using recycled polycarbonate and ABS feedstock [92]. Olawumi et al. reported that the efficiency of various recycling approaches in recycling polymers preserves up to 90% of their tensile

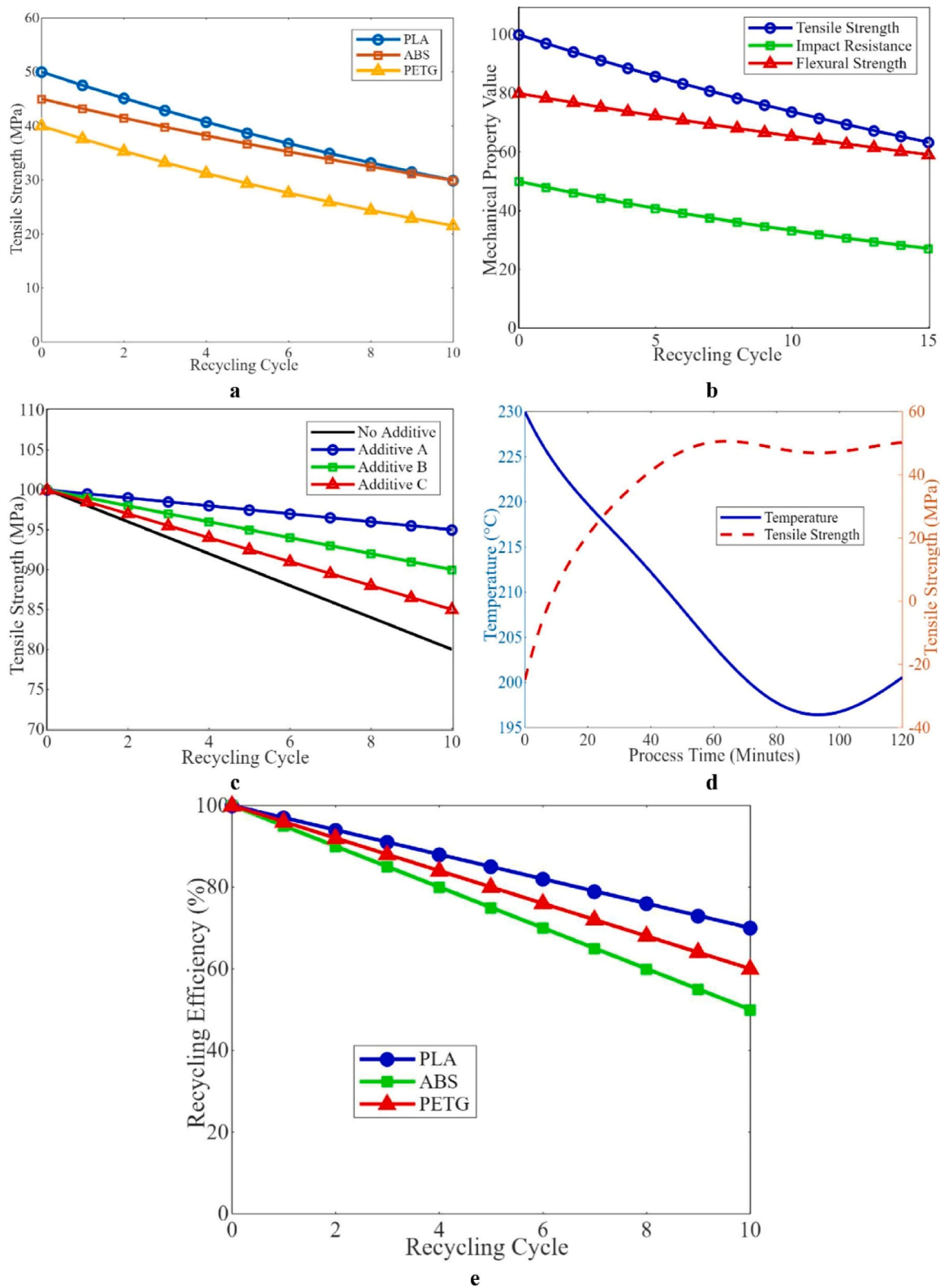


Fig. 10. (a) Impact of recycling cycles on tensile strength, (b) degradation of mechanical properties over recycling cycles, (c) efficiency of additives in tensile strength over recycling cycles and (d) temperature variations in the FDM process and material quality (e) recycling efficiency across over PLA, ABS, and PETG polymer types [88].

strength after the first cycle, deteriorating to 80% after three cycles [88]. As shown in Fig. 10, each polymer (PLA, ABS, and PETG) exhibits a downward trend in tensile strength. In contrast, PLA and ABS follow nearly parallel degradation paths, while PETG displays a lower tensile strength with a steeper decline. This features the effect of repetitive recycling on the mechanical integrity of generally used polymers in AM processes. This demonstrates how various polymers withstand the recycling process, which is essential for developing sustainable practices and lowering environmental impact and carbon footprint. The closed-loop mechanical recycling of PLA for FDM printing has been investigated, and its environmental performance has been assessed using life cycle assessment (LCA) [93]. The PLA was only able to undergo two cycles of the AM process due to the observed deterioration in the viscosity values. Besides the recycling of plastics, alternative sources of materials, such as natural wastes, marine industry wastes, agricultural by-products, and construction debris, can be utilised in the AM process [94,95].

The main reasons for polymer degradation and subsequent changes in melt flow rate (MFR) and tensile impact strength during the recycling are the high temperatures and shear forces used during the recycling process. Since 80–90% of recycling costs can be determined during the design stage, circular product design and design for recycling (DfR) allows the circularity to easily generate products and their recycling by maintaining the end-of-life protocols. The DfR makes the design to be

more recyclable in terms of sustainability and environmental concerns. Kalinke et al. developed bespoke AM filaments from recycled PLA (65 wt %), 10 wt% polyethylene succinate (PES), 15 wt% carbon black (CB), and 10 wt% of carboxylated multi-walled carbon nanotubes and exhibits enhanced electrochemical performance with an electrochemically active area of $(2.11 \pm 0.03) \text{ cm}^2$ compared to $(1.19 \pm 0.19) \times 10^{-3} \text{ cm}^2 \text{ s}^{-1}$, and $(1.35 \pm 0.02) \text{ cm}^2$ for an identical commercial filament [96]. This work highlights the utilization of recycled feedstock in AM to enhance healthcare sector by improving end-product sustainability. Romani et al. reported the mechanical behavior of recycled PLA feedstock which shows that elastic modulus remains constant, with a minimal decrease of -1.0% whereas the ultimate tensile strength further decreased by -16.4% after six extrusion cycles respectively [97]. Korey et al. recycled carbon fiber (CF) filaments ABS based molds and uses the granulates used as feedstocks for AM processes [98]. The resultant elastic modulus after mechanical recycling exhibits a decrement of 10% in the printing direction and of 10% transverse to printing direction which could be attributed to the reduced fiber content and molecular weight of polymer. As shown on Fig. 11 a, 39% reduction in fiber length was observed between the virgin pellets (249.1 μm) and printed virgin sample (147.2 μm) and the distribution of fiber lengths specifies an increased occurrence of longer fibers (150–200 μm) in the granulate sample as compared to the print from virgin material (100–150 μm). Since there is a potential loss of small fibers during granulation, thermal

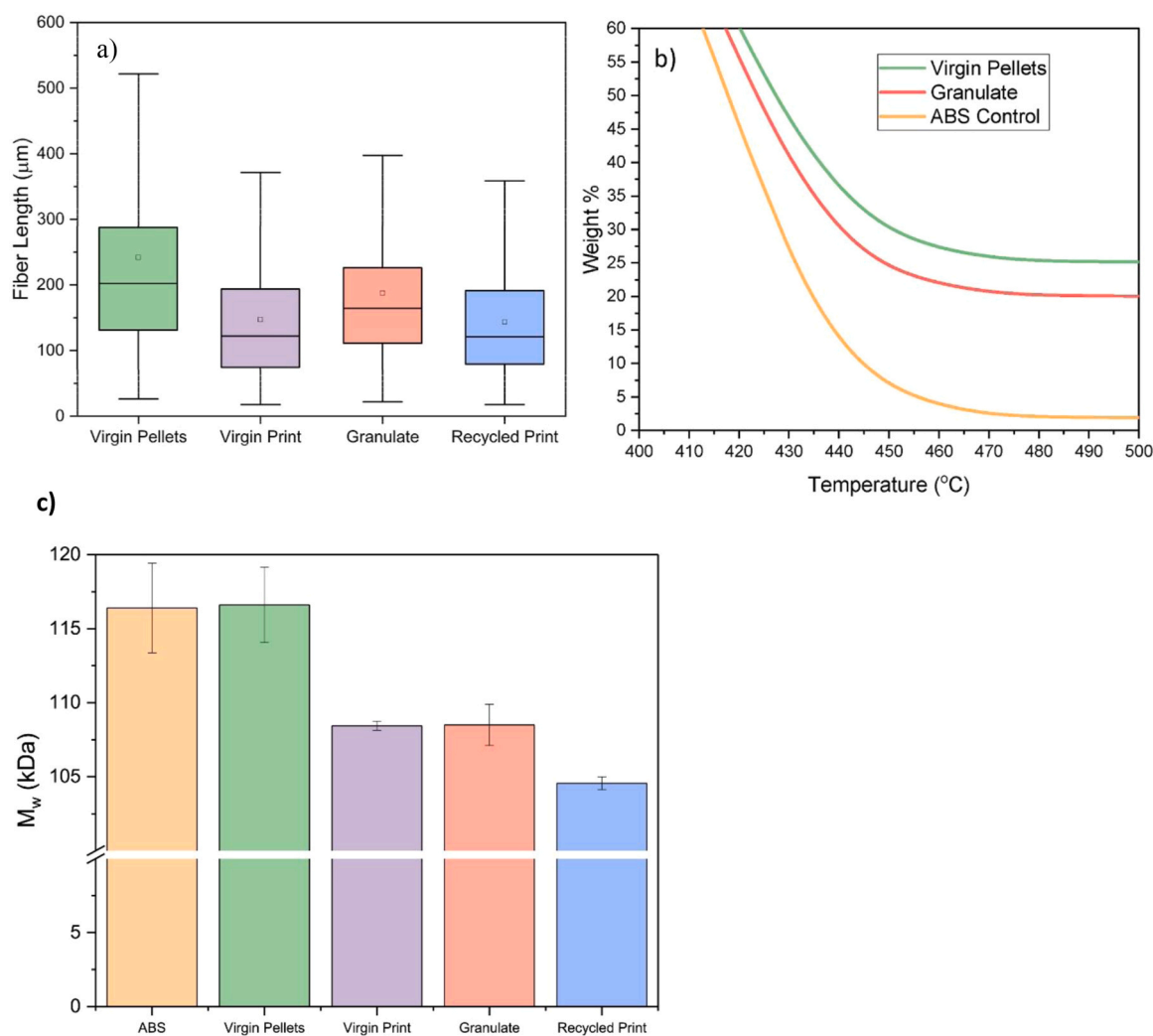


Fig. 11. a) fiber length analysis of pellets, pellet print, granulate, and granulate print. b) thermal degradation of CF content in CF-ABS samples by TGA. c) gel permeation chromatography showing the significant reduction in M_w in virgin print compared to virgin CF-ABS pellets and a significant reduction in M_w in recycled print sample as compared to recycled CF-ABS granulate. Reprinted with permission from Elsevier [99].

degradation analysis (Fig. 11 b) shows no significant changes in thermal stability associated with granulation and indicates a 13.5% reduction in the CF content in the granulate compared to the virgin pellets. Moreover, gel permeation chromatography reports a significant reduction (7.0%, $p < 0.05$) and (3.6%, $p < 0.05$) in molecular weight (Mw) of ABS matrix after the first and second print respectively as shown in Fig. 11 c.

A major challenge with the consumption of recycled materials in the AM is the inconsistency in their properties, which can considerably impact the print quality and mechanical integrity of the final products. Establishing standardised procedures for recycling and material preparation will avoid such inconsistencies. The use of natural fibres introduces additional challenges, including impurities, variable particle sizes, and moisture absorption, which can lead to nozzle blockages, weak interlayer bonding, and surface flaws in printed components. The inferior mechanical performance of the composites made from recycled or natural waste materials compared to conventional alternatives is another challenge. This highlights the need for continued research to optimise formulations and refine processing parameters to improve critical properties, such as thermal resistance, tensile strength, and interfacial bonding [95]. Incorporating 3D printing and recycling is a crucial approach to implementing sustainable industrial processes and promoting the recirculation of materials. By using recycled materials, environmental impact can be reduced, circularity promoted, and resources conserved. Nevertheless, the materials should be rigorously assessed to ensure they will yield safe and high-quality products.

6. Life cycle assessment of additively manufactured polymer composites

Life cycle assessment (LCA) is an internationally standardised method based on ISO 14040 and 14044 standards used to calculate the environmental impact of a product or a process across its different life cycle stages. The four main steps of LCA are (i) goal and scope definition, (ii) inventory analysis, (iii) impact assessment, and (iv) interpretation. [89,99–101]. In additive manufacturing, such assessments aid decision-making for cost-effective and scalable production by identifying environmental hotspots such as energy use, emissions and waste generation [102]. Kokar *et al.* recently reviewed the existing LCA studies related to AM and highlighted some of the limitations, such as predominant emphasis on environmental sustainability without sufficient attention to economic and social aspects; lack of integration of part quality and mechanical performance into sustainability evaluations; minimal coverage of post-manufacturing life cycle stages; and inadequate exploration of how different product-related variables influence the overall sustainability [6]. Existing studies of polymer and polymer composite AM materials differ substantially in their goals and scopes, including functional unit (e.g., per part, per kg of material), system boundaries (e.g., cradle-to-gate, cradle-to-grave), background electricity mixes, and chosen impact assessment methods. As a result, absolute impact values are not directly comparable across studies, and normalizing results is challenging due to different system boundaries and functional units. Several studies have analyzed the environmental impact of AM technologies, with LCA being the methodology of choice. However, the available data on the application of LCA in medical application of polymer and polymer composites, is still scarce.

Recently, several studies [92,101,103–106] have explored the ecological footprint of AM technologies, with LCA being the main analytical approach. However, the available data on the application of LCA in medical AM is still relatively scarce. Armstrong *et al.* performed a bottom-up LCA to evaluate the environmental impact of precast concrete molds made from conventional wood, and AM molds from wood floor-PLA (WF/PLA), and recycled carbon fiber-ABS (CF/ABS) [103]. The LCA encompassed all life cycle stages from raw material sources to the on-site use of molds for a comparative evaluation of AM and traditional life cycle energy and carbon emissions. The results showed that traditional wood molds had the lowest environmental impact, which is

attributed to the limited processing required after wood is harvested, unlike composite materials that undergo more intensive processing. As shown in Fig. 12 (a), the cost of each AM mold of CF/ABS and WF/PLA decreases with increased use of recycled material and the number of times the material is recycled. Wood-based alternatives offer a significantly lower environmental impact if the AM molds are not recycled. Nonetheless, the sustainability of wood depends on several external factors not addressed in the study, such as land-use change, geographic origin, and transportation logistics to the construction site. The cost reduction for the WF/PLA mold is less significant than that of CF/ABS. The material costs and life cycle energy and life cycle carbon emission for both AM molds are substantially reduced, as shown in Fig. 12 (b-d), with recycled CF/ABS approaching the impact of primary WF/PLA. However, the available data on the application of LCA in the medical application of AM is still relatively scarce [107]. In a recent report [6] a total of 59 studies were analysed exclusively using LCA, focusing on the environmental aspects of AM processes. Additionally, 12 reports examined environmental and economic dimensions by integrating LCA with life cycle costing (LCC). In contrast, only five studies addressed the social sustainability of AM through the social life cycle assessment (S-LCA) approach to assess the social dimension of AM adoption from a life cycle perspective. The S-LCA methodology measures and compares the products manufactured by a conventional technique with an AM technique in terms of their performance and the impact of production and development [84]. Table 3 synthesizes LCA, LCC, S-LCA, and LCSA studies on polymer-composite AM by aligning the material system, AM technology, goal and scope, functional unit, and system boundaries, and impact assessment method. It identifies the hotspots in the study and synthesizes main findings which allow for in-depth comparison of the studies.

The findings in Table 3 show major methodological challenges when considering comparison of the studies. The studies differ significantly in system boundaries (cradle-to-gate vs. cradle-to-grave, inclusion or exclusion of the use phase), functional units (per specimen, per device, per kg, per treatment), geographical location and electricity mix, and the LCIA methods and indicators applied. End-of-life is treated very unevenly, as several studies are cradle-to-grave only, others assume simple landfill or incineration, and only a few explicitly model polymer or fibre recycling. These choices can shift contributions between production and end-of-life stages and strongly influence whether AM or conventional manufacturing appears favourable, complicating any direct cross-study comparison and making it risky to generalise from isolated case studies [6,83–85,103,105,106,108].

Addressing these challenges will require more harmonised and AM specific LCA practice. At minimum, future studies should: (i) clearly define and justify functional units that reflect the service provided, (ii) adopt transparent and comparable system boundaries that consistently include or justify exclusion of use and end of life stages, (iii) report electricity mixes and key inventory assumptions explicitly, and (iv) adopt a limited set of recommended impact methods and indicators for AM to facilitate comparison. Modular or parametric LCA frameworks tailored to AM could further improve comparability by enabling scenario analyses across design variants, build strategies, and energy mixes within a single, consistent model, rather than across unrelated case studies.

The limited number of studies that have integrated all three sustainability pillars by jointly applying LCA, LCC, and S LCA to AM, especially in the context of AM and polymer composites, underlines how rare holistic assessments still are. There is a clear need to systematically extend the analysis of AM beyond isolated environmental or techno economic metrics and towards life cycle sustainability assessment (LCSA). LCSA is particularly important as AM technologies mature and diversify in terms of feedstock, process routes, and application domains, because it provides a structured way to track how innovations in materials (e.g., biobased polymers, recycled composites), processes (e.g., higher energy efficiency, reduced support, hybrid manufacturing), and

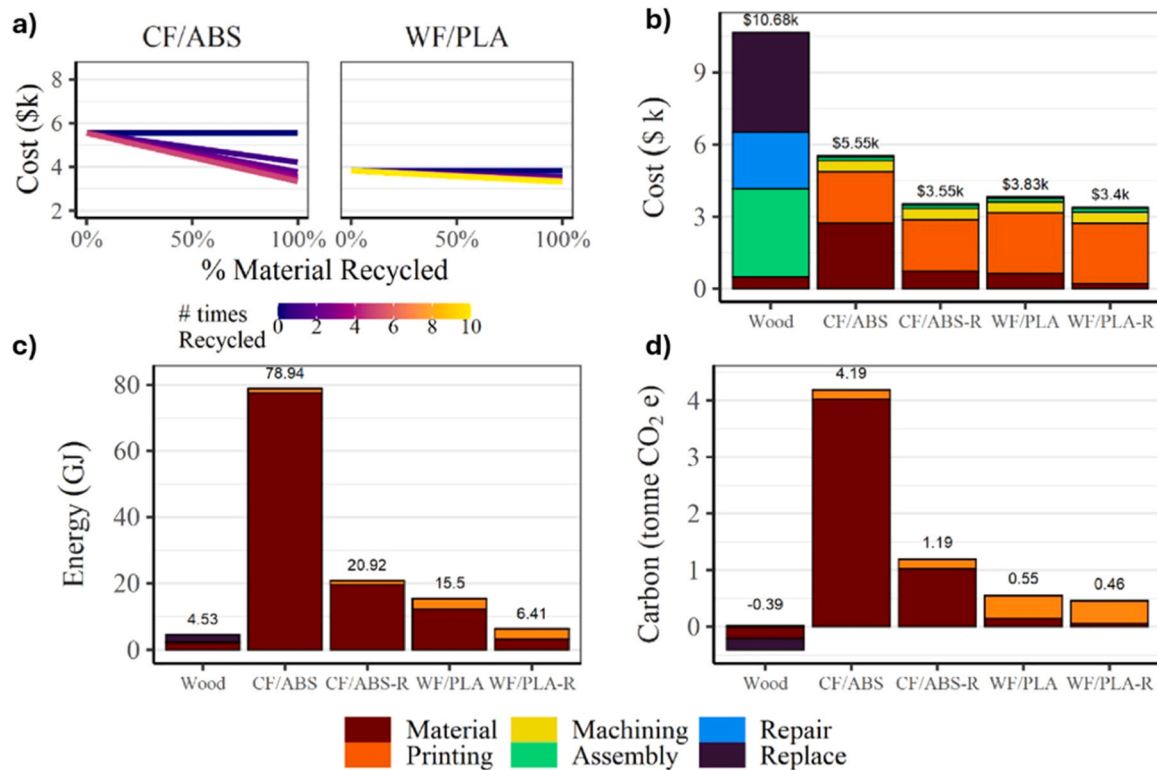


Fig. 12. Impact of the materials recycled, and the number of times recycled on lifecycle cost (a), life cycle cost comparison (b), energy (c), and carbon emissions (d) for conventional wood, CF/ABS, and WF/PLA to the recycled AM feedstock (R indicates mold materials are 90% material recycled 5 times).

product designs (e.g., lightweighting, functional integration) simultaneously influence climate and resource use, total cost of ownership, and social aspects such as worker safety, job quality, and user benefits. Many AM processes have higher specific energy use than conventional routes, especially when designs are not optimised or loads are low. Although AM routes can have higher upfront energy and sometimes higher material impacts, they can compensate through longer service life, reduced scrap, and improved functionality, particularly for geometrically complex or customised parts [6].

7. Safety aspects of additively manufactured polymer composites

The safety concerns in the AM of polymer composites regarding emissions and exposure during printing and post-processing which arise primarily from ultrafine particles (UFPs) and material-specific volatile organic compounds (VOCs), with process route, material choice, and ventilation strongly influencing risks [109–111]. To evaluate UFP emissions during 3D printing, which can contribute to inflammatory and cardiovascular effects, Zontek et al. monitored working environments in a poorly ventilated and a well-ventilated laboratory [112]. They demonstrated substantially lower concentrations of chemical gases and metallic elements in the well-ventilated laboratory and found that in printer aerosol mass concentrations ranged from 0.1 to 83.3 $\mu\text{g}/\text{m}^3$ depending on the phase (heating, printing, cooling, opening doors), with the heating phase emitting the highest values. Keeping the printer door closed in an enclosed setup reduced particle number and mass concentrations, and thus operator exposure, by about 95% [112].

A modelling analysis for a 45 m^3 furnished office with a typical ventilation rate of 1 h^{-1} showed that a single desktop printer operating continuously with high emitting filament combinations could elevate indoor concentrations to approximately 58 000 particles/ cm^3 , 244 $\mu\text{g}/\text{m}^3$ caprolactam, 150 $\mu\text{g}/\text{m}^3$ styrene and 6 $\mu\text{g}/\text{m}^3$ lactide. Although these concentrations remain below 8 h occupational limits for styrene and

caprolactam, they significantly increase indoor pollutant loads and justify caution when operating multiple printers or using styrene and nylon-based filaments in enclosed or poorly ventilated spaces [113]. The primary chemical safety concern is the emission of toxic VOCs such as toluene, ethylbenzene, aldehydes and styrene, which are particularly relevant for ABS based composites and methacrylate rich resins. Baguley et al. systematically compiled VOC measurements from both filament and resin bed desktop printers and compared them with health-based guidance values and workplace exposure limits. For resin bed systems, VOCs most frequently associated with adverse health effects included 2 butanone, 2 hydroxyethyl methacrylate, 2 hydroxypropyl methacrylate, acetone, 2 methyl 2,4 pentanediol, and styrene, typically reported at time weighted average concentrations from a few $\mu\text{g}/\text{m}^3$ up to the low mg/m^3 range depending on printer type, resin formulation, and ventilation. Although most reported concentrations were below British Workplace Exposure Limits and other occupational guideline values, repeated exposure to complex VOC mixtures, particularly in small, poorly ventilated rooms or for vulnerable groups, may still pose irritation, neurotoxic or sensitisation risks. For example, 2 hydroxypropyl methacrylate, a known skin and respiratory irritant, has been reported in the range of 2–31.2 $\mu\text{g}/\text{m}^3$ or 40–2800 $\mu\text{g}/\text{h}$, depending on the unit used [110,112,114].

Emissions and associated risks are highest for unenclosed printers using ABS, nylon or composite filaments, or methacrylate rich resins, particularly in home, office or small lab environments with limited ventilation; they are substantially reduced when low emission materials (e.g. PLA or other low odor formulations) are combined with enclosures, filtration and adequate room ventilation. Conservative risk management for AM polymer composites should therefore prioritise low emission materials when performance permits or low odor, reduced emission formulations, as well as enclosed printers with effective filtration and local exhaust, and process optimisation to minimise temperatures and print times without compromising part quality. These measures complement material specific toxicological and biocompatibility evaluation

Table 3

Recent LCA, LCC and SLCA, and LCSA studies polymer composites in AM. The table highlights the diversity of functional units, system boundaries, and impact assessment methods.

Type of study	Material (s)AM technology	Goal, scope, FU	Study details	Hotspots in the system	Main findings	Reference
LCA	Materials PA6, PA6-CF, ABS AM Technology FFF	Goal and Scope: Environmental impacts of numerical modelling vs. 3D-printing FU: One standard tensile testing specimen	System Boundary: Cradle-to-gate Stages: filament production, 3D printing, and mechanical testing. LCIA: TRACI 2.1 midpoint impact categories studied global warming potential (GWP), acidification potential (AP), eutrophication potential (EP), ozone depletion potential (ODP), and fossil fuel depletion (FFD) Databases and datasets: GaBi with proprietary and regional datasets. Attributional approach Electricity mix: Qatar grid mix EO: Not included/specified	Electrical energy used during the FFF process. Mechanical testing stage for categories of GWP, AP, and EP. Experimental design materials consumed contributed considerably to ODP.	The environmental impact of numerical modeling was significantly lower than that of the experimental approach for all impact categories considered.	[89]
LCA	Materials PLA, ABS, PETG filaments AM Technology FDM / material extrusion	Goal: Environmental impacts of 3D-printed soap holder using PLA, ABS, and PETG Scope: environmental impacts due to material and electricity use FU: one soap holder (51 cm ³)	System boundary: Cradle-to-cradle Stages: raw material extraction, filament production, printing, passive use, recycling via re-extrusion. LCIA: ReCiPe 2016 midpoint (8 categories) climate change, fossil depletion, freshwater ecotoxicity, human toxicity, ozone depletion, particulate matter formation, terrestrial acidification, and water depletion and endpoint (human health, ecosystem, resources) Databases and datasets: Umberto NXT software with Ecoinvent database attribution. Attributional approach Electricity mix: Indian grid mix EO: Recycling	Recycling phase has been found to have the highest environmental impact. The raw-material phase is associated with high water depletion and ecotoxicity for PLA.	PETG had the lowest environmental impact in all midpoint and end-point categories. ABS material is the least environmentally friendly. PLA material has the highest negative impacts on water depletion and freshwater ecotoxicity.	[104]
LCA	Materials PA6 and PVA AM Technology Arburg Plastic Freeforming (APF) and FFF	Goal and Scope: Assessment of environmental effects of lightweight design methods on a finger splint. FU: one Patient-Specific Finger Splint	System boundary: Cradle-to-gate Stages: including material production, printing (machine LC and energy), plates/consumables. LCIA: ReCiPe 2016 endpoint categories Databases and datasets: Parametric LCA models based on prior APF and FFF frameworks; SimaPro/ecoinvent and PEF datasets for PA6 and PVA; attributional Electricity mix: not directly	Machine life cycle Energy use Build time	The marginal contribution of material is used to environmental impacts. The impacts increase with the building time per part. The findings are connected to the geometry of the investigated case studies.	[107]

(continued on next page)

Table 3 (continued)

Type of study	Material (s)AM technology	Goal, scope, FU	Study details	Hotspots in the system	Main findings	Reference
LCA, LCC	Materials: rCFPA12 and vCFPA12 AM Technology: FDM	Goal and Scope: The comparison of virgin and recycled PA12 polymer carbonfiber's life cycle FU: The production of the specimen that exhibits a maximum strain equal to 2.5% when subjected to a tensile load of 1.1 kN Using the vCF and rCF composite materials	specified although the location is specified as Bologna (Italy) EoL: Not included/specified System boundary: Cradle-to-gate.Stages: manufacturing of specimens including processes dispersion, filaments fabrication, drying, andPrinting LCIA: Impact 2002 + method focusing on six critical mid-points such as Aquatic acidification (A.A.),carcinogens (C), ionizing radiation (I. R.), non-renewable energy(NREC), ozone layer depletion (O.D.), and global warming potential(GWP) Databases and datasets: The European Life Cycle Database (ELCD) data for productionof polyacrylonitrile (PAN) Literature data on the environmental impact of the recycling process andrecycled carbon fiber composites Literature data of the polyamide-6 (PA6) was adopted to model the raw material in terms of the PA12The Ecoinvent transportation datasets Electricity mix: not specified EoL: Not included/specified	Manufacturing the specimensusing both composites has the most significant influence on humanshealth compared to the other categories for both composites.rCF has a lower impact onthe environmental damage category than vCF due to the lowermass required for the rCF-PA12 sample to achieve the desired stiffness. Human health is the primary environmental damage endpoint resulting from the manufacturing of the specimens using rCF and vCF-reinforced polyamide. The printing process of vCF required approximately4.6 MJ of power, which is about 61.5% of the overall energy needed.In contrast, the energy required to produce the raw materials ofvCF is about 0.2 MJ, which is about only 2.6% of the overallenergy needed to manufacture the vCF-PA12 specimen.	The rCF has less impact on all environmental categories ofNREC, OLD, I.R., GWP, A.A., and C compared to vCF. When rCF was used in polymer composites, it reduced energy usage, greenhouse gas emissions, and waste production.The non-renewable energyrequired for manufacturing rCF-PA12 is approximately 12% less than the energy needed for manufacturing the sample using vCF-PA12. To achieve equivalent stiffness, the GWP due to the manufacturing ofspecimens using rCF are approximately 8.8% lower than vCF (0.52 and 0.57 kg CO ₂ eq). Cost-wise rCF has a 50% lower cost than vCF.	[106]
LCA, LCC	Materials: woodflour (WF)-PLArecycled carbon fiber-ABS AM Technology: not specified	Goal and Scope: The comparison of cycle cost, energy, and carbon emissions of molds for precast concrete made from WF/PLA, wood, and CF/ABS molds. FU: per project basisThe production of the required quantity of a specific style of window frame (75 pours as baseline case).	System boundary: Cradle to gate with use phase also includedStages: the initial mold construction and subsequent repairs or additional molds required are included LCIA: Cumulative Energy Demand (CED)TRACI 2.1 methodFocus was on life cycle energy and carbon emissions Databases and datasets: Data taken from literatureEcoinvent 3.5	Direct labor costs account for 68% ofthe out-of-the-gate cost.The LCC of wood mold is heavily dominated by labor costs. Capital expenses represent 38% of the total life cycle costs for CF/ABSand 55% for WF/PLA.Materials costs represent 50% (\$2740) of CF/ABS costs and 17% for WF/PLA. The hostpost for CED is material in	wood molds are substantially less impactful if AM molds are not recycledAM composites hold several advantages when time is a key factor.Conventional wood molds have the lowest life cycle energy and carbon emissions of the three types of molds, as shown.The life cycle energy is 2100 MJ/mold for materials andmanufacturing phases, compared to 15,400 MJ/mold for WF/PLA and78,800 MJ/mold for CF/ABS composite.	[103]

(continued on next page)

Table 3 (continued)

Type of study	Material (s)AM technology	Goal, scope, FU	Study details	Hotspots in the system	Main findings	Reference
LCA	Materials: PLA Technology: FDM	Goal and Scope: The comparison of the end-of-life alternatives of a 3D printed product FU: 1 kg of 3D printable PLA	System boundary: End-of-life stage LCIA: ReCiPe method Databases and datasets: GaBi software Primary data, including energy use and mass losses, that related to 3D printing processing and reprocessing were determined experimentally. Secondary data LCI datasets taken from GaBi software Electricity mix: CN Electricity grid mix EoL modeling <ul style="list-style-type: none"> • Close-looped (mechanical) recycling • landfill • incineration 	the case of CF/ABS and WF/PLA composite. The hotspots for carbon emissions are materials for CF/ABS and printing for WF/PLA composite. Landfilling is associated with negative environmental impacts. Environmental savings are associated with closed-loop recycling and incineration.	The most significant environmental benefits can be achieved in closed-loop recycling. Landfilling is the end-of-life option with the highest environmental burdens. Closed-loop recycling achieves the most significant environmental savings in the category of freshwater eutrophication potential, because a huge amount of water use in PLA polymerisation is avoided. Comparatively speaking, combustion of PLA is more environmentally friendly, yet economically unvia	[93]
LCA	Materials: polyamide (PA) matrix reinforced with carbon fibers (CFs) or glass fibers AM Technology: FFF	Goal and Scope: The evaluation and comparison of the environmental behavior of CarbonPA and GlassPA composite materials FU: The production of a tensile specimen that exhibits a maximum strain equal to 2.55% when subjected to a tensile load of 3.1 kN with length of 170 mm	System boundary: Cradle-to-grave LCIA: CED and GWP Databases and datasets: Ecoinvent database considering European glass manufacturing industry data Electricity mix: not specified EoL Landfill disposal	Polyamide production represents the main contribution to the total impacts of the filaments, accounting for more than 50–80% of the final material CED values, depending on the scenarios.	The raw material production phases have shown similar environmental impacts for both scenarios, with variations of less than 10%. The electric energy use during the 3D printing process decreases with an increase in thickness. CarbonPA is more eco-friendly when subjected to tensile loads on 3D printed components. GlassPA has a lower environmental impact when 3D printed components must withstand flexural stress. 22% higher total life cycle energy use is associated with the GlassPA composite (6.19 MJ) compared to CarbonPA.	[108]
LCA	Materials: PETG copolymer AM Technology: Digital Light Processing (DLP)	Goal and Scope: The quantification of the environmental burdens associated with DLP and thermoforming for producing dental aligners FU: 40 dental aligners with packaging (an average complete set needed for the treatment)	System boundary: Cradle-to-gate Stages: the production of precursors from raw materials, logistics, and the production of aligners. LCIA: EF 3.1 method with impact categories Acidification, Climate change, Energy resources, Ozone depletion, and Eutrophication, freshwater, marine and terrestrial Databases and datasets: OpenLCA v1.11.0 software Ecoinvent v3.9 database Literature data for processes not available in the	For thermoforming, the primary impact in most categories is a result of the raw materials used, followed by the energy required. For DLP, the hotspots in categories of CC and Energy resources are materials needed and energy. In the category of acidification, the hotspots are raw material and packaging.	Thermoforming process was associated with a higher environmental impact in all categories considered. In the category of Ozone depletion, DLP had a 98% lower impact compared to the thermoforming process. DLP is associated with a lower impact on water use as only a small amount of water is required for removing residuals of resin.	[105]

(continued on next page)

Table 3 (continued)

Type of study	Material (s)AM technology	Goal, scope, FU	Study details	Hotspots in the system	Main findings	Reference
SLCA	<p>Materials:ABS (orthosis)PLA for the prototypes andFilaflex™ for the final product (prosthesis)AM Technology:Fused Filament Deposition (FFD)</p>	<p>Goal and Scope:To assess the social impact of AM in healthcareSector by studying two cases, related to the development,production and use of a medical product producedby AM (orthosis and prosthesis). FU:Not specified</p>	<p>Ecoinvent databaseAttributional Allocation cut-offElectricity mix: electricity, low voltage, residual mix electricity, low voltage Cutoff, U (IT)IoL:Not specified/included System boundary: Each case is evaluated throughthe performance comparison of AM production with the conventional production contextCase study methodology considering end-users, users' needs, production processes and professionals involved.LCIA:Adapted method developed by Franze and Ciroth (2011). The study evaluates each case through comaprison of AM with conventional technology and not the country/region contextThe impact categories anaysed are Working Conditions (WC), Health and Safety (HS), Human Rights (HR), Socio-Economic Repercussions (SER), and Governance (G). Databases and datasets:Primary data (focus groups, unstructured interviews, ethnographic observations) Secondary data (clinical patient information, literature data, product specifications) Electricity mix: /EoL: / System boundary: Gate-to-graveStages: material processing, manufacturing, sterilization, packaging, storage, transportation, and disposalLCIA:LCA: ReCiPe 2016 Midpoint (H) Social analysis:</p> <ul style="list-style-type: none"> • Worker heathl and safety • Job satisfaction in workers • Customer satisfaction <p>Life cycle unit costEntropy weight method (EWM) for measuring the</p>	<p>Negative effects are associated with 'Respect for intellectual property rights' in the case of AM prothesis and orthosis manufacturing.</p>	<p>The main positive impacts are associated with the creation of locally specialized jobs, as well as general technological and economic development.The results indicate an increase in the adoption and continued use of medical devices by patients, resulting in faster reintegration into society.</p>	[84]
LCSA	<p>Materials:PLA pallets and aluminaAM Technology:FDM</p>	<p>Goal and Scope:The identification of the environmental impact and hotspots of scaffold supply chain where FDM is compared with traditional manufacturing (TM) process (freeze drying).FU:A product life cycle supply chain. Unit product cost for LCC.</p>	<p>Electricity mix: /EoL: / System boundary: Gate-to-graveStages: material processing, manufacturing, sterilization, packaging, storage, transportation, and disposalLCIA:LCA: ReCiPe 2016 Midpoint (H) Social analysis:</p> <ul style="list-style-type: none"> • Worker heathl and safety • Job satisfaction in workers • Customer satisfaction <p>Life cycle unit costEntropy weight method (EWM) for measuring the</p>	<p>The material processing stage consumes the highest percentage of total cost (40.37% and 31.29% for AM and TM networks, respectively). The major cause of the environmental effect is related to the electricity input, i.e. primary energy required. The fabrication step has a higher impact on GWP ecotoxicity, human toxicity, and</p>	<p>The primary energy demand for fabrication is ~11 times higher for the traditional manufacturing process. TM compared to AM. IEnergy usecost for material processing and fabrication are higher for traditional manufacturing processes. Labour cost is higher for AM due to design process and material dependency, which may create a psychosocial risk in the workplace. EWM was used to assess sustainability indexes. AM has higher environmental sustainability index, TM has The overall composite sustainability index for AM is 0.9271 and 0.0136 for TM route, indicating AM is a more sutainable method.</p>	[83]

(continued on next page)

Table 3 (continued)

Type of study	Material (s)AM technology	Goal, scope, FU	Study details	Hotspots in the system	Main findings	Reference
			sustainability index. Databases and datasets: Simapro software ecoinvent database Primary inventory data was collected experimentally during production stage Questionnaires for the industry and academia experts for SLCA Electricity mix: Indian with dataset Electricity, medium voltage {IN-Northern grid} market for electricity, medium voltage APOS, UDisposal of plastic, polyethylene and waste paperboard EO: Disposal Disposal cost of scaffold packaging only.	resource use categories.		

as in biomedical applications, safety and efficacy are evaluated through biocompatibility analyses, which assess interactions of materials with biological systems, and toxicological assessment provides detailed information on cell viability, proliferation and functional activity in contact with additively manufactured scaffolds [115,116].

In line with these findings, Romanowski et al. reviewed 50 studies covering the topic of emissions of 3D printing, focusing on FFF and reported released amounts of particles ranged from 107 to 1012 particles/min. The measured particle number concentrations ranged from 103 to 105 particles/cm³ during printing with PLA filament and from 104 to 106 particles/cm³ during ABS printing [117]. Azimi et al. analysed different printers and filament materials from several manufacturers and classified filaments into low and high VOC emitters, showing that the same nominal filament type from different manufacturers can differ substantially in both the amount and composition of VOC emissions [113]. Their results confirmed that lactide dominates VOC emissions from PLA filaments, styrene from ABS, and caprolactam from nylon and certain wood/brick composite filaments [ref]. These findings suggest that filament material and manufacturer strongly influence both UFP and VOC emission rates and that low-emission PLA-type filaments should be preferred over ABS, nylon and certain composites in poorly ventilated or non-industrial settings whenever mechanical performance allows.

Further research is needed to elucidate the mechanisms of toxic matter formation across various AM techniques, but existing evidence already supports basic exposure-reduction strategies. Comprehensive management of printing protocols (using the lowest effective print temperatures, minimising print times and support structures), combined with enclosed printers, effective filtration, and good room ventilation, can reduce exposures. Consumers and users should be made aware of emissions and mitigation options, such as operating printers in a separate, well-ventilated room and avoiding prolonged operation in small, enclosed spaces. The use of standardised testing methods is crucial for comparing printers and materials; in this context, ANSI/CAN/UL 2904 (“Standard Method for Testing and Assessing Particle and Chemical Emissions from 3D Printers”) provides harmonised measurement and assessment protocols for particle and VOC emissions and is a useful reference when selecting testing procedures and benchmarking emission performance [117].

8. Summary and perspectives

This work systematically reviews the additive manufacturing (3D and 4D printing) of polymer composites, focusing on fabrication techniques, composite types, and their advantages and applications from a sustainable perspective. The AM processes of polymer composites by 3D and 4D printing techniques have been clearly described with recent progress in studies. Various fabrication methods, along with their corresponding advantages and limitations, are reviewed. The sustainability, recyclability, life cycle analyses, safety and environmental aspects of polymer composites manufactured by AM techniques have been systematically reviewed.

The key conclusions and perspectives from this review are outlined below.

1. The sustainability of additively manufactured polymer composites is evaluated from a social, environmental, and economic perspective. The polymers and fillers used in the composites should also be eco-friendly and sustainable, with minimal environmental impact during their processing. However, AM still relies on energy, material consumption, waste generation, and health risks due to the emission of pollutants. This challenge can be addressed by utilising eco-friendly reagents and feedstocks derived from renewable and biodegradable resources, as well as by incorporating the intended design structures and the capability to reprocess materials, thereby supporting the green revolution and a circular economy. To achieve this, it is essential to assess net waste reduction and associated costs compared to traditional manufacturing methods. In this way, AM technology offers sustainable manufacturing in terms of resource efficiency and an extended product life, with a reconfigured value chain. AM offers notable environmental advantages, including reduced material waste, better energy utilisation, and the possibility of localised production, which can decrease transportation-related emissions.
2. By using recycled materials in the AM processes, the environmental impact can be reduced, circularity promoted, and resources conserved. However, recyclability should be meaningful as the final products ensure the desired yield and quality. The consumption of recycled materials in the AM processes is limited mainly due to the

inconsistencies in their properties, which affect the print quality and mechanical integrity of the final products. The inferior mechanical performance of products from recycled or natural waste feedstocks primarily arises from the presence of impurities, particle size variations, and moisture absorption. The speed limitations of AM techniques and the higher costs associated with AM machinery pose another challenge in recycling. To overcome this, an established standardisation procedure for recycling should be implemented. Future research on AM should be focused on optimising formulations and refining processing parameters to achieve recyclability.

- To promote sustainable development and gain a holistic understanding of AM's sustainability potential, it is essential to evaluate technological advancements in materials, processes, and applications through a complete life cycle assessment using LCA, LCC, and SLCA. Future research should focus on conducting a comprehensive life cycle assessment of AM processes, encompassing economic, environmental, and social sustainability dimensions. The post-production phases and end-of-life modeling should also be included in the assessments. Furthermore, machine-learning predictive models should be implemented to estimate the quality and sustainability of AM-based polymer composites, thereby eliminating the need for time-consuming conventional processes. In this way, post-production, utilisation, and end-of-life phases of the AM product life cycle are used to gain a comprehensive view of the environmental, economic, and social impacts of AM products.
- Mechanical performance of polymer composites fabricated by AM techniques is an important parameter to evaluate their sustainability assessments by checking their dimensional accuracy compared with conventional products. The quality and mechanical performance of AM parts can be adversely affected by the presence of defects or poor mechanical properties, which can negatively impact the product's service life and performance, ultimately increasing the life cycle cost. Future research on AM will be focused on developing more environmentally friendly materials with cleaner manufacturing techniques to reduce the harmful effects of synthetic and petroleum-based polymers. Biodegradable polymers and eco-friendly natural fibres reinforced composites should reduce the environmental impact and promote sustainability. Such composites still require more advancement in terms of feedstock filament, agglomeration and orientation of fillers, and matrix-filler adhesion.
- Further research is needed to elucidate the safety and health risks due to the emission of toxic substances across various AM techniques. To overcome this, a comprehensive management of printing protocols should be implemented in conjunction with the use of biodegradable materials in manufacturing processes. Environmentally friendly machinery and safety equipment to ensure personal protection should also be implemented. Future research of AM-based polymer composites should focus on safety, sustainability, degradation behaviour, long-term performance, and the lifecycle of materials used. New eco-friendly materials and corresponding technologies should be introduced.

CRediT authorship contribution statement

Simon Muhic: Writing – review & editing, Supervision, Resources, Project administration, Funding acquisition. **Jelena Topić Božić:** Writing – original draft, Visualization, Validation, Software, Methodology, Investigation, Formal analysis, Data curation. **Yasir Beeran Pottathara:** Writing – review & editing, Writing – original draft, Visualization, Validation, Supervision, Software, Methodology, Investigation, Formal analysis, Data curation, Conceptualization.

Declaration of Competing Interest

The authors declare that they have no known competing financial interests or personal relationships that could have appeared to influence

the work reported in this paper.

Acknowledgement

The research was co-funded by the Slovenian Research and Innovation Agency (ARIS) through the annual work program of Rudolfov Science and Technology Center, Novo Mesto.

Data availability

Data will be made available on request.

References

- X. Wang, M. Jiang, Z. Zhou, J. Gou, D. Hui, 3D printing of polymer matrix composites: a review and prospective, *Compos. B Eng.* 110 (2017) 442–458, <https://doi.org/10.1016/j.compositesb.2016.11.034>.
- G.N. Levy, R. Schindel, J.P. Kruth, Rapid manufacturing and rapid tooling with layer manufacturing (LM) technologies, state of the art and future perspectives, *CIRP Ann.* 52 (2003) 589–609, [https://doi.org/10.1016/S0007-8506\(07\)60206-6](https://doi.org/10.1016/S0007-8506(07)60206-6).
- B.H. Jared, M.A. Aguilo, L.L. Beghini, B.L. Boyce, B.W. Clark, A. Cook, B.J. Kaehr, J. Robbins, Additive manufacturing: toward holistic design, *Scr. Mater.* 135 (2017) 141–147, <https://doi.org/10.1016/j.scriptamat.2017.02.029>.
- D. Puppi, F. Chiellini, Biodegradable polymers for biomedical additive manufacturing, *Appl. Mater. Today* 20 (2020) 100700, <https://doi.org/10.1016/j.apmt.2020.100700>.
- A. Haleem, M. Javaid, S. Rab, R.P. Singh, R. Suman, L. Kumar, Significant potential and materials used in additive manufacturing technologies towards sustainability, *Sustain. Oper. Comput.* 4 (2023) 172–182, <https://doi.org/10.1016/j.susoc.2023.11.004>.
- S. Kokare, J.P. Oliveira, R. Godina, Life cycle assessment of additive manufacturing processes: a review, *J. Manuf. Syst.* 68 (2023) 536–559, <https://doi.org/10.1016/j.jmsy.2023.05.007>.
- Y. Wang, A. Ahmed, A. Azam, D. Bing, Z. Shan, Z. Zhang, M.K. Tariq, J. Sultana, R.T. Mushtaq, A. Mehboob, C. Xiaohu, M. Rehman, Applications of additive manufacturing (AM) in sustainable energy generation and battle against COVID-19 pandemic: The knowledge evolution of 3D printing, *J. Manuf. Syst.* 60 (2021) 709–733, <https://doi.org/10.1016/j.jmsy.2021.07.023>.
- J. Izdebska-Podsiady, Chapter 3 - Classification of 3D printing methods, in: J.B. T.-P. for 3D P. Izdebska-Podsiady (Ed.), *Plastics Design Library*, William Andrew Publishing, 2022, pp. 23–34, <https://doi.org/10.1016/B978-0-12-818311-3.00009-4>.
- J. Pierre, F. Iervolino, R.D. Farahani, N. Piccirelli, M. Lévesque, D. Therriault, Material extrusion additive manufacturing of multifunctional sandwich panels with load-bearing and acoustic capabilities for aerospace applications, *Addit. Manuf.* 61 (2023) 103344, <https://doi.org/10.1016/j.addma.2022.103344>.
- X. Wu, A. Rastogi, N. Gotawala, M.A. Pandol, Y. Zhu, H.Z. Yu, Shear-driven solid-state additive manufacturing of aerospace aluminum on impurity contaminated surfaces, *Mater. Des.* 256 (2025) 114312, <https://doi.org/10.1016/j.matdes.2025.114312>.
- C. Boursier Niutta, A. Tridello, G. Barletta, N. Gallo, A. Baroni, F. Berto, D. S. Paolino, Defect-Driven topology optimization for fatigue design of additive manufacturing structures: Application on a real industrial aerospace component, *Eng. Fail. Anal.* 142 (2022) 106737, <https://doi.org/10.1016/j.engfailanal.2022.106737>.
- H. Lin, Z. Li, M. Fu, H. Yi, H. Zhang, R. Li, Ultrasonic rolling-enhanced additive manufacturing of IN718 superalloy: Microstructural refinement and mechanical property improvement through variable power modulation, *Addit. Manuf.* 109 (2025) 104891, <https://doi.org/10.1016/j.addma.2025.104891>.
- F.T. Jahromi, M. Nikzad, K. Prasad, J. Norén, M. Isaksson, A. Arian, I. Sbarski, Additive manufacturing of polypropylene micro and nano composites through fused filament fabrication for automotive repair applications, *Polym. Adv. Technol.* 34 (2023) 1059–1074, <https://doi.org/10.1002/pat.5952>.
- D. Chauhan, A.P. Singh, A. Chauhan, R. Arora, Sustainable supply chain: An optimization and resource efficiency in additive manufacturing for automotive spare part, *Sustain. Futures* 9 (2025) 100563, <https://doi.org/10.1016/j.sfr.2025.100563>.
- P.C. Priarone, A.R. Catalano, L. Settineri, Additive manufacturing for the automotive industry: on the life-cycle environmental implications of material substitution and lightweighting through re-design, *Progress. Addit. Manuf.* 8 (2023) 1229–1240, <https://doi.org/10.1007/s40964-023-00395-x>.
- M. Vlkovsky, A. Ilkstrom-Kravcov, T. Slajs, The Implementation of Additive Technologies in the Army and Key Personnel Training, *Int. Conf. Comput. Nat. Sci. Biomed. Eng. (COMCONF) 2024* (2024) 136–141, <https://doi.org/10.1109/COMCONF63340.2024.00027>.
- H. Su Cho, J. Keun Cha, H. Sung Kim, A. Basyir, S. Hyung Kim, Additive manufacturing of multidimensional Al/PVDF-based energetic composite structures featuring enhanced safety and combustion performance, *J. Ind. Eng. Chem.* 137 (2024) 216–224, <https://doi.org/10.1016/j.jiec.2024.03.007>.
- M. Petousis, N. Michailidis, V. Papadakis, A. Argyros, M. Spiridakis, N. Mountakis, J. Valsamos, N.K. Nasikas, A. Moutsopolou, N. Vidakis, Enhanced engineering

- and biocidal polypropylene filaments enabling melt reduction of AgNO₃ through PVP agent: A scalable process for the defense industry with MEX additive manufacturing, *Def. Technol.* 44 (2025) 52–66, <https://doi.org/10.1016/j.dt.2024.09.007>.
- [19] N. Vidakis, N. Michailidis, M. Petousis, N.K. Nasikas, V. Saltas, V. Papadakis, N. Mountakis, A. Argyros, M. Spiridaki, I. Valsamos, Multifunctional HDPE/Cu biocidal nanocomposites for MEX additive manufactured parts: Perspectives for the defense industry, *Def. Technol.* 38 (2024) 16–32, <https://doi.org/10.1016/j.dt.2024.03.004>.
- [20] P. Singh, H. Baniyasi, S. Gupta, R. Ghosh, S. Shaikh, J. Seppälä, A. Kumar, 3D-printed cellulose nanocrystals and gelatin scaffolds with bioactive cues for regenerative medicine: Advancing biomedical applications, *Int. J. Biol. Macromol.* 278 (2024) 134402, <https://doi.org/10.1016/j.ijbiomac.2024.134402>.
- [21] C. Wu, B. Wan, A. Entezari, J. Fang, Y. Xu, Q. Li, Machine learning-based design for additive manufacturing in biomedical engineering, *Int. J. Mech. Sci.* 266 (2024) 108828, <https://doi.org/10.1016/j.ijmecs.2023.108828>.
- [22] W.E.C. Martínez, Y.K.R. Acosta, A.V. Reyes Acosta, R.E.D. de León Gómez, A. R. Patel, D.K. Verma, C.N. Aguilar, Advances in Poly(lactic acid)-based composites as a promising biomaterial for food packaging and biomedical Applications: Reinforcement strategies, functional enhancements, and future research directions, *Sustain. Mater. Technol.* 45 (2025) e01560, <https://doi.org/10.1016/j.susmat.2025.e01560>.
- [23] Q. Zhang, C. Sun, J. Zheng, L. Wang, C. Liu, D. Li, Mechanical behaviour of additive manufactured PEEK/HA porous structure for orthopaedic implants: Materials, structures and manufacturing processes, *J. Mech. Behav. Biomed. Mater.* 163 (2025) 106848, <https://doi.org/10.1016/j.jmbm.2024.106848>.
- [24] Y.B. Pottathara, V. Kokol, Effect of nozzle diameter and cross-linking on the micro-structure, compressive and biodegradation properties of 3D printed gelatin/collagen/hydroxyapatite hydrogel, *Bioprinting* 31 (2023) e00266, <https://doi.org/10.1016/j.bprint.2023.E00266>.
- [25] R. Agarwal, J. Singh, V. Gupta, Predicting the compressive strength of additively manufactured PLA-based orthopedic bone screws: A machine learning framework, *Polym. Compos.* 43 (2022) 5663–5674, <https://doi.org/10.1002/pc.26881>.
- [26] A. Haleem, M. Javaid, Role of CT and MRI in the design and development of orthopaedic model using additive manufacturing, *J. Clin. Orthop. Trauma.* 9 (2018) 213–217, <https://doi.org/10.1016/j.jcot.2018.07.002>.
- [27] J. Ma, X. Zhou, Z. Ye, X. Tong, Z. Chen, Q. Xia, T. Wang, Y. Jin, Y. Li, J. Lin, Z. Zhao, C. Wen, L. Zhu, β -spodumene-doped lithium disilicate glass-ceramics via additive manufacturing for dental applications, *J. Mater. Sci. Technol.* 247 (2026) 289–301, <https://doi.org/10.1016/j.jmst.2025.04.082>.
- [28] H. Yousef, B.T. Harris, E.N. Elathamna, D. Morton, W.-S. Lin, Effect of additive manufacturing process and storage condition on the dimensional accuracy and stability of 3D-printed dental casts, *J. Prosthet. Dent.* 128 (2022) 1041–1046, <https://doi.org/10.1016/j.prosdent.2021.02.028>.
- [29] B. Aktas, R. Das, H.G. Aktas, E. Uyar, S. Yalcin, B. Ergin, Z. Celik, E.O. Ulas, Additive manufacturing of TiO₂-doped 3Y-ZrO₂ ceramics via DLP-3D printing for dental implant applications: Enhanced mechanical strength, biocompatibility, and antibacterial performance, *J. Alloy. Compd.* 1037 (2025) 182246, <https://doi.org/10.1016/j.jallcom.2025.182246>.
- [30] L. Wang, L. Yao, W. Tang, R. Dou, Effect of Fe₂O₃ doping on color and mechanical properties of dental 3Y-TZP ceramics fabricated by stereolithography-based additive manufacturing, *Ceram. Int.* 49 (2023) 12105–12115, <https://doi.org/10.1016/j.ceramint.2022.12.062>.
- [31] A. Bhardwaj, 3D Printing and Additive Manufacturing: Recent Trends in Fashion and Textile Production, in: R. Nayak, H. Truong, R. Pal (Eds.), *Use of Digital and Advanced Technologies in the Fashion Supply Chain*, Springer Nature Singapore, Singapore, 2025, pp. 223–246, https://doi.org/10.1007/978-981-97-7528-6_9.
- [32] L. Yang, J. Meng, T. Xue, Y. Wang, G. Shi, X. Gao, C. Zhi, Application of 3D printing cellulose fabrics based on cotton fibers in the textile and fashion industry, *Addit. Manuf.* 81 (2024) 104000, <https://doi.org/10.1016/j.addma.2024.104000>.
- [33] Q. Yu, M. Zhang, A.S. Mujumdar, J. Li, AI-based additive manufacturing for future food: potential applications, challenges and possible solutions, *Innov. Food Sci. Emerg. Technol.* 92 (2024) 103599, <https://doi.org/10.1016/j.ifset.2024.103599>.
- [34] F.D.C. Siacor, Q. Chen, J.Y. Zhao, L. Han, A.D. Valino, E.B. Taboada, E. B. Caldon, R.C. Advincola, On the additive manufacturing (3D printing) of viscoelastic materials and flow behavior: From composites to food manufacturing, *Addit. Manuf.* 45 (2021) 102043, <https://doi.org/10.1016/j.addma.2021.102043>.
- [35] J.I. Lipton, M. Cutler, F. Nigl, D. Cohen, H. Lipson, Additive manufacturing for the food industry, *Trends Food Sci. Technol.* 43 (2015) 114–123, <https://doi.org/10.1016/j.tifs.2015.02.004>.
- [36] S.A.V. Dananjaya, V.S. Chevali, J.P. Dear, P. Potluri, C. Abeykoon, 3D printing of biodegradable polymers and their composites – Current state-of-the-art, properties, applications, and machine learning for potential future applications, *Prog. Mater. Sci.* 146 (2024) 101336, <https://doi.org/10.1016/j.pmatsci.2024.101336>.
- [37] K. Agrawal, A.R. Bhat, Advances in 3D printing with eco-friendly materials: a sustainable approach to manufacturing, *RSC Sustain.* 3 (2025) 2582–2604, <https://doi.org/10.1039/D4SU00718B>.
- [38] N. Yarangatti, A. Patnaik, A review on additive manufacturing of polymers composites, *Mater. Today Proc.* 44 (2021) 4150–4157, <https://doi.org/10.1016/j.matpr.2020.10.490>.
- [39] I.S.O. Astm, ISO/ASTM 52900:2015(en) Additive manufacturing — General principles — Terminology, (n.d.).
- [40] O. Luzanin, V. Guduric, I. Ristic, S. Muhic, Investigating impact of five build parameters on the maximum flexural force in FDM specimens – a definitive screening design approach, *Rapid Prototyp. J.* 23 (2017) 1088–1098, <https://doi.org/10.1108/RPJ-09-2015-0116>.
- [41] N. Vidakis, D. Kalderis, N. Michailidis, V. Papadakis, N. Mountakis, A. Argyros, M. Spiridaki, A. Moutsoulou, M. Petousis, Environmentally friendly polylactic acid/ferro-nickel slag composite filaments for material extrusion 3D printing: A comprehensive optimization of the filler content, *Mater. Today Sustain.* 27 (2024) 100881, <https://doi.org/10.1016/j.mtsust.2024.100881>.
- [42] B.B. Mansingh, J.S. Binoj, Z.Q. Tan, W.L.E. Wong, T. Amornsakchai, S.A. Hassan, K.L. Goh, Characterization and Performance of Additive Manufactured Novel bio-waste Polylactic acid eco-friendly Composites, *J. Polym. Environ.* 31 (2023) 2306–2320, <https://doi.org/10.1007/s10924-023-02758-5>.
- [43] N.A. Eleessawy, A. El Shakhs, M. Fahmy El-Saka, M.E. Yousef, B.A.B. Yousef, M. A. Malek Ali, Sustainable and eco-friendly 3D printing filament fabricated from different recycled solid wastes and evaluate its impact on interior and furniture design, *Results Eng.* 23 (2024) 102428, <https://doi.org/10.1016/j.rineng.2024.102428>.
- [44] S. Xia, S. Li, Z. Li, H. Li, H. Fu, A. Wang, Z. Zhu, H. Zhang, Eco-friendly material extrusion 3D printing for fabricating W-Ni-Fe lattices with improved compressive resistance, *Addit. Manuf.* 92 (2024) 104399, <https://doi.org/10.1016/j.addma.2024.104399>.
- [45] M. Pelanconi, S. Bottacin, M. Caccia, A. Ortona, Y. Li, Effect of crystalline Si₃N₄ fillers on the mechanical strength and thermal stability of complex SiCN(O) ceramic architectures produced by powder bed fusion and densified via polymer infiltration and pyrolysis, *Open. Ceram.* 24 (2025) 100846, <https://doi.org/10.1016/j.oceram.2025.100846>.
- [46] M. Yan, X. Tian, Mechanical property of powder bed fusion printed carbon fiber reinforced polyetheretherketone and enhanced interlayer strength by post-processing, *Polym. Compos.* 45 (2024) 13578–13588, <https://doi.org/10.1002/pc.28719>.
- [47] Y. Hou, M. Gao, R. An, W.S. Tey, B. Li, J. Chen, L. Zhao, K. Zhou, Surface modification of oriented glass fibers for improving the mechanical properties and flame retardancy of polyamide 12 composites printed by powder bed fusion, *Addit. Manuf.* 62 (2023) 103195, <https://doi.org/10.1016/j.addma.2022.103195>.
- [48] W.-C. Lin, J.-F. Tang, C.-C. Cheng, C.-C. Kuo, W.-H. Hung, Development of low-shrinkage eco-friendly composite materials for the DLP 3D printing technique, *Mater. Adv.* 6 (2025) 1889–1898, <https://doi.org/10.1039/D4MA00722K>.
- [49] Y. Yu, L. Xu, S. Liu, G. Gu, Y. Chen, H. Yuan, H.-C. Kuan, J. Liu, Q. Meng, J. Ma, Eco-friendly, mechanically robust, weather-resistant and rapidly cured polyurea elastomer synthesized by vat photopolymerization 3D printing, *Compos. Part. A Appl. Sci. Manuf.* 196 (2025) 108985, <https://doi.org/10.1016/j.compositesa.2025.108985>.
- [50] G. Colucci, F. Di Stefano, F. Sacchi, M. Licciardello, C. Tonda-Turo, L. Lavagna, M. Messori, Bio-based polymer composites obtained by vat photopolymerization of photocurable resins modified with biochar as sustainable filler, *Compos. Part. A Appl. Sci. Manuf.* 198 (2025) 109102, <https://doi.org/10.1016/j.compositesa.2025.109102>.
- [51] H. Baniyasi, D. Puttonen, R. Abidnejad, S. Jayaprakash, J. Partanen, E. Lizundia, J. Niskanen, Biochar-reinforced polyamide 12 composites for sustainable selective laser sintering 3D printing: Performance enhancement and carbon footprint reduction, *Chem. Eng. J.* 519 (2025) 165502, <https://doi.org/10.1016/j.cej.2025.165502>.
- [52] A.I.B. Idriss, C.-M. Yang, J. Li, Y. Guo, J. Liu, A.A.A. Abdelmagid, G.A. Ahmed, H. Zhang, Influence of particle size on the mechanical performance and sintering quality of peanut husk powder/PES composites fabricated through selective laser sintering, *Polymers* 15 (2023), <https://doi.org/10.3390/polym15193913>.
- [53] R. Ajdary, N. Kretschmar, H. Baniyasi, J. Trifol, J.V. Seppälä, J. Partanen, O. J. Rojas, Selective Laser Sintering of Lignin-Based Composites, *ACS Sustain. Chem. Eng.* 9 (2021) 2727–2735, <https://doi.org/10.1021/acsschemeng.0c07996>.
- [54] G. Colucci, F. Lupone, F. Bondioli, M. Messori, 3D printing of PBAT-based composites filled with agro-wastes via selective laser sintering, *Eur. Polym. J.* 215 (2024) 113197, <https://doi.org/10.1016/j.eurpolymj.2024.113197>.
- [55] V. Kokol, Y.B. Pottathara, M. Mihelčić, L.S. Perše, Rheological properties of gelatine hydrogels affected by flow- and horizontally-induced cooling rates during 3D cryo-printing, *Colloids Surf. A Physicochem. Eng. Asp.* 616 (2021) 126356, <https://doi.org/10.1016/j.colsurfa.2021.126356>.
- [56] Y.B. Pottathara, V. Kokol, Additive manufacturing techniques for designing advanced scaffolds for bone tissue engineering. *Nanotechnology-Based Additive Manufacturing*, John Wiley & Sons, Ltd, 2023, pp. 435–454, <https://doi.org/10.1002/9783527835478.ch15>.
- [57] S. Das, L. Cherwoo, A. Kundu, S. Kumar, A. Sharma, N. Thombare, A. P. Bhonekar, Bio-inspired conductive ink: Harnessing plant based binder for customizing electrochemical, rheological and printing applications, *Mater. Today Commun.* 40 (2024) 109927, <https://doi.org/10.1016/j.mtcomm.2024.109927>.
- [58] E. Erfanian, R. Moaref, R. Ajdary, K.C. Tam, O.J. Rojas, M. Kamkar, U. Sundararaj, Electrochemically synthesized graphene/TEMPO-oxidized cellulose nanofibrils hydrogels: Highly conductive green inks for 3D printing of robust structured EMI shielding aerogels, *Carbon N. Y* 210 (2023) 118037, <https://doi.org/10.1016/j.carbon.2023.118037>.
- [59] H. Rao C, B.K.S.V.L. Varaprasad, S. Goel, Direct Ink Writing as an Eco-Friendly PCB Manufacturing Technique for Rapid Prototyping, *Fourth Int. Conf. Electr.*

- Comput. Commun. Technol. (ICECCT) 2021 (2021) 1–7, <https://doi.org/10.1109/ICECCT52121.2021.9616903>.
- [60] Dan Liu, Di Wu, Yi Xiao, Rui Zhan, Xin-Rong Zeng, Ke-Ke Yang, Direct-Ink-Writing Printing of Shape Memory Cross-Linked Networks from Biomass-Derived Small Molecules, *Sustain. Polym. Energy* 2 (2024) 10008, <https://doi.org/10.70322/spe.2024.10008>.
- [61] F. Wang, M. Jiang, Y. Pan, Y. Lu, W. Xu, Y. Zhou, 3D Printing photo-induced lignin nanotubes/polyurethane shape memory composite, *Polym. Test.* 119 (2023) 107934, <https://doi.org/10.1016/j.polymertesting.2023.107934>.
- [62] J. Bai, C. Han, Y. Gao, D. Wang, S. Yang, G. Liu, H. Sun, S. Gao, W. Yin, W. Song, UV-assisted direct ink writing of near-infrared light-responsive shape memory plant-based resin bone scaffold, *Biomater. Adv.* 177 (2025) 214381, <https://doi.org/10.1016/j.bioadv.2025.214381>.
- [63] T. Wu, S. Sugiarto, R. Yang, T. Sathasivam, U.A. Weerasinghe, P.L. Chee, O. Yap, G. Nyström, D. Kai, From 3D to 4D printing of lignin towards green materials and sustainable manufacturing, *Mater. Horiz.* 12 (2025) 2789–2819, <https://doi.org/10.1039/D4MH01680G>.
- [64] J.A. Dicks, C. Woolard, Leveraging Itaconic Acid in Microcrystalline Cellulose Reinforced Shape Memory Photopolymers for Sustainable 4D Printing, *Macromol. Mater. Eng.* n/a (n.d.) e00227, <https://doi.org/https://doi.org/10.1002/mame.202500227>.
- [65] Mohd Danish, P. Vijay Anirudh, C. Karunakaran, V. Rajamohan, A.T. Mathew, K. Koziol, V.K. Thakur, C. Kannan, A.S.S. Balan, 4D printed stereolithography printed plant-based sustainable polymers: Preliminary investigation and optimization, *J. Appl. Polym. Sci.* 138 (2021) 50903, <https://doi.org/10.1002/app.50903>.
- [66] S. Li, Z. Li, S. Mei, X. Chen, B. Ding, Y. Zhang, W. Zhao, X. Zhang, Z. Cui, P. Fu, X. Pang, M. Liu, 4D Printed Thermoplastic Polyamide Elastomers with Reversible Two-Way Shape Memory Effect, *Adv. Mater. Technol.* 8 (2023) 2202066, <https://doi.org/10.1002/admt.202202066>.
- [67] D. Wu, Y.-M. Leng, C.-J. Fan, Z.-Y. Xu, L. Li, L.-Y. Shi, K.-K. Yang, Y.-Z. Wang, 4D Printing of a Fully Biobased Shape Memory Copolyester via a UV-Assisted FDM Strategy, *ACS Sustain. Chem. Eng.* 10 (2022) 6304–6312, <https://doi.org/10.1021/acssuschemeng.2c00721>.
- [68] E.J. Shin, J.H. Son, H.S. Lee, S. Lee, Manufacturing of Conductive Filaments for 3D/4D Printing through In Situ Polymerization of Biobased Thermoplastic Polyurethane/Multiwall Carbon Nanotube Composites, *ACS Appl. Polym. Mater.* 6 (2024) 1751–1762, <https://doi.org/10.1021/acscapm.3c02558>.
- [69] X. Wan, H. Wei, F. Zhang, Y. Liu, J. Leng, 3D printing of shape memory poly(d,l-lactide-co-trimethylene carbonate) by direct ink writing for shape-changing structures, *J. Appl. Polym. Sci.* 136 (2019) 48177, <https://doi.org/10.1002/app.48177>.
- [70] M. Zhou, Y. Tian, M.L.S. Nai, H.J. Qi, K. Zhou, 4D printing of multiscale filler-reinforced thermoplastic polyurethane nanocomposites with electro-activated shape memory properties, *Virtual Phys. Prototyp.* 20 (2025) e2474537, <https://doi.org/10.1080/17452759.2025.2474537>.
- [71] M.A. Yousefi, D. Rahmatabadi, M. Baniassadi, M. Bodaghi, M. Baghani, 4D Printing of Multifunctional and Biodegradable PLA-PBAT-Fe3O4 Nanocomposites with Supreme Mechanical and Shape Memory Properties, *Macromol. Rapid Commun.* 46 (2025) 2400661, <https://doi.org/10.1002/marc.202400661>.
- [72] P. Feng, R. Zhao, F. Yang, S. Peng, H. Pan, C. Shuai, Co-continuous structure enhanced magnetic responsive shape memory PLLA/TPU blend fabricated by 4D printing, *Virtual Phys. Prototyp.* 19 (2024) e2290186, <https://doi.org/10.1080/17452759.2023.2290186>.
- [73] P. Fu, H. Li, J. Gong, Z. Fan, A.T. Smith, K. Shen, T.O. Khalfalla, H. Huang, X. Qian, J.R. McCutcheon, L. Sun, 4D printing of polymers: Techniques, materials, and prospects, *Prog. Polym. Sci.* 126 (2022) 101506, <https://doi.org/10.1016/j.progpolymsci.2022.101506>.
- [74] D. Rahmatabadi, A. Bayati, M. Khajepour, K. Mirasadi, I. Ghasemi, M. Baniassadi, K. Abrinia, M. Bodaghi, M. Baghani, Poly(ethylene terephthalate) glycol/carbon black composites for 4D printing, *Mater. Chem. Phys.* 325 (2024) 129737, <https://doi.org/10.1016/j.matchemphys.2024.129737>.
- [75] S. Ali, M. Alshihabi, L. Beard, I. Deiah, S. Pervaiz, Dual-Stimuli Responsive and Sustainable PLA/APHA/TPU Blend for 4D Printing, *Macromol. Rapid Commun.* n/a (n.d.) e00414, <https://doi.org/https://doi.org/10.1002/marc.202500414>.
- [76] B. Narupai, P.T. Smith, A. Nelson, 4D Printing of Multi-Stimuli Responsive Protein-Based Hydrogels for Autonomous Shape Transformations, *Adv. Funct. Mater.* 31 (2021) 2011012, <https://doi.org/10.1002/adfm.202011012>.
- [77] B. Li, G. Bartolini Torres, B. Martin, N. Taylor, E. Barbu, A. Christie, A. Heise, Polycaprolactone-Itaconic Acid Resins for Additive Manufacturing of Environmentally Degradable 3D and 4D Materials by Thiol-ene Photopolymerization, *Macromolecules* 58 (2025) 8887–8897, <https://doi.org/10.1021/acs.macromol.5c01310>.
- [78] M. Jurinovič, M. Veseta, A. Sabalina, P.E.S. Silva, A. Linarts, H. Baniassadi, J. Vapaavuori, S. Gaidukovs, Sustainable 4D printable biobased shape memory polymers with linear tunability and multistimuli actuation for advanced applications, *Small Sci.* 5 (2025) 2500104, <https://doi.org/10.1002/ssmc.202500104>.
- [79] S. Mei, J. Wang, Z. Li, B. Ding, S. Li, X. Chen, W. Zhao, Y. Zhang, X. Zhang, Z. Cui, P. Fu, X. Pang, M. Liu, 4D printing of polyamide 1212 based shape memory thermoplastic polyamide elastomers by selective laser sintering, *J. Manuf. Process.* 92 (2023) 157–164, <https://doi.org/10.1016/j.jmapro.2023.02.033>.
- [80] H. Ouyang, X. Li, X. Lu, H. Xia, Selective laser sintering 4D printing of dynamic cross-linked polyurethane containing Diels-Alder bonds, *ACS Appl. Polym. Mater.* 4 (2022) 4035–4046, <https://doi.org/10.1021/acscapm.2c00565>.
- [81] G. Taddese, S. Durieux, E. Duc, Sustainability performance indicators for additive manufacturing: a literature review based on product life cycle studies, *Int. J. Adv. Manuf. Technol.* 107 (2020) 3109–3134, <https://doi.org/10.1007/s00170-020-05249-2>.
- [82] G. Chyr, J.M. DeSimone, Review of high-performance sustainable polymers in additive manufacturing, *Green. Chem.* 25 (2023) 453–466, <https://doi.org/10.1039/D2GC03474C>.
- [83] N. Choudhary, V. Sharma, P. Kumar, Sustainability assessment framework of biomedical scaffolds: additive manufacturing versus traditional manufacturing, *J. Clean. Prod.* 418 (2023) 138118, <https://doi.org/10.1016/j.jclepro.2023.138118>.
- [84] B. Soares, I. Ribeiro, G. Cardeal, M. Leite, H. Carvalho, P. Peças, Social life cycle performance of additive manufacturing in the healthcare industry: the orthosis and prosthesis cases, *Int. J. Comput. Integr. Manuf.* 34 (2021) 327–340, <https://doi.org/10.1080/0951192X.2021.1872100>.
- [85] D. Rejeski, F. Zhao, Y. Huang, Research needs and recommendations on environmental implications of additive manufacturing, *Addit. Manuf.* 19 (2018) 21–28, <https://doi.org/10.1016/j.addma.2017.10.019>.
- [86] G. Prasad, H. Arunav, S. Dwight, M.B. Ghosh, A. Jayadev, D.I. Nair, Advancing sustainable practices in additive manufacturing: a comprehensive review on material waste recyclability, *Sustainability* 16 (2024), <https://doi.org/10.3390/su162310246>.
- [87] B.I. Oladapo, J.F. Kayode, P. Karagiannidis, N. Naveed, H. Mehrabi, K. O. Ogundipe, Polymeric composites of cubic-octahedron and gyroid lattice for biomimetic dental implants, *Mater. Chem. Phys.* 289 (2022) 126454, <https://doi.org/10.1016/j.matchemphys.2022.126454>.
- [88] M.A. Olawumi, B.I. Oladapo, T.O. Olugbade, Evaluating the impact of recycling on polymer of 3D printing for energy and material sustainability, *Resour. Conserv. Recycl.* 209 (2024) 107769, <https://doi.org/10.1016/j.resconrec.2024.107769>.
- [89] A. Al Rashid, S.A. Khan, M. Koç, Life cycle assessment on fabrication and characterization techniques for additively manufactured polymers and polymer composites, *Clean. Environ. Syst.* 12 (2024) 100159, <https://doi.org/10.1016/j.cesys.2023.100159>.
- [90] E. Sanchez-Rexach, T.G. Johnston, C. Jehanno, H. Sardon, A. Nelson, Sustainable materials and chemical processes for additive manufacturing, *Chem. Mater.* 32 (2020) 7105–7119, <https://doi.org/10.1021/acs.chemmater.0c02008>.
- [91] B. Peeters, N. Kiratli, J. Semeijn, A barrier analysis for distributed recycling of 3D printing waste: taking the maker movement perspective, *J. Clean. Prod.* 241 (2019) 118313, <https://doi.org/10.1016/j.jclepro.2019.118313>.
- [92] A. Romani, M. Levi, J.M. Pearce, Recycled polycarbonate and polycarbonate/acrylonitrile butadiene styrene feedstocks for circular economy product applications with fused granular fabrication-based additive manufacturing, *Sustain. Mater. Technol.* 38 (2023) e00730, <https://doi.org/10.1016/j.susmat.2023.e00730>.
- [93] P. Zhao, C. Rao, F. Gu, N. Sharmin, J. Fu, Close-looped recycling of polylactic acid used in 3D printing: an experimental investigation and life cycle assessment, *J. Clean. Prod.* 197 (2018) 1046–1055, <https://doi.org/10.1016/j.jclepro.2018.06.275>.
- [94] S. Palaniyappan, N.K. Sivakumar, V. Sekar, Sustainable approach to the revalorization of crab shell waste in polymeric filament extrusion for 3D printing applications, *Biomass-- Convers. Biorefin* 14 (2024) 15721–15738, <https://doi.org/10.1007/s13399-023-03795-9>.
- [95] A. Yousaf, A. Al Rashid, R. Polat, M. Koç, Potential and challenges of recycled polymer plastics and natural waste materials for additive manufacturing, *Sustain. Mater. Technol.* 41 (2024) e01103, <https://doi.org/10.1016/j.susmat.2024.e01103>.
- [96] C. Kalinke, R.D. Crapnell, E. Sigley, M.J. Whittingham, P.R. de Oliveira, L. C. Brazaca, B.C. Janegitz, J.A. Bonacin, C.E. Banks, Recycled additive manufacturing feedstocks with carboxylated multi-walled carbon nanotubes toward the detection of yellow fever virus cDNA, *Chem. Eng. J.* 467 (2023) 143513, <https://doi.org/10.1016/j.cej.2023.143513>.
- [97] A. Romani, L. Perusin, M. Ciurnelli, M. Levi, Characterization of PLA feedstock after multiple recycling processes for large-format material extrusion additive manufacturing, *Mater. Today Sustain.* 25 (2024) 100636, <https://doi.org/10.1016/j.mtsust.2023.100636>.
- [98] M. Korey, M.L. Rencheck, H. Tekinalp, S. Wasti, P. Wang, S. Bhagia, R. Walker, T. Smith, X. Zhao, M.E. Lamm, K. Copenhaver, U. Vaidya, S. Ozcan, Recycling polymer composite granulate/regrid using big area additive manufacturing, *Compos. B Eng.* 256 (2023) 110652, <https://doi.org/10.1016/j.compositesb.2023.110652>.
- [99] J. Topić Božić, U. Fric, A. Čikić, S. Muhič, Life cycle assessment of using firewood and wood pellets in Slovenia as two primary wood-based heating systems and their environmental impact, *Sustainability* 16 (2024), <https://doi.org/10.3390/su16041687>.
- [100] J.T. Božić, A. Čikić, S. Muhič, Environmental impact of Slovenian and Croatian electricity generation using an hourly production-based dynamic life cycle assessment approach, *Energies* 18 (2025), <https://doi.org/10.3390/en18184826>.
- [101] J. Dimnik, J. Topić Božić, A. Čikić, S. Muhič, Impacts of high PV penetration on Slovenia's electricity grid: energy modeling and life cycle assessment, *Energies* 17 (2024), <https://doi.org/10.3390/en17133170>.
- [102] C.S. Gonzalez, A. Basdeo, F.A. Cruz Sanchez, C. Nouvel, J.M. Pearce, H. Boudaoud, Strategies for recycling multi-material polymer blends for additive manufacturing, *Sustain. Mater. Technol.* 44 (2025) e01430, <https://doi.org/10.1016/j.susmat.2025.e01430>.

- [103] K.O. Armstrong, D. Kamath, X. Zhao, M.L. Rencheck, H. Tekinalp, M. Korey, D. Hun, S. Ozcan, Life cycle cost, energy, and carbon emissions of molds for precast concrete: Exploring the impacts of material choices and additive manufacturing, *Resour. Conserv. Recycl.* 197 (2023) 107117, <https://doi.org/10.1016/j.resconrec.2023.107117>.
- [104] R. Kumar, H. Sharma, C. Saran, T.S. Tripathy, K.S. Sangwan, C. Herrmann, A comparative study on the life cycle assessment of a 3D printed product with PLA, ABS & PETG materials, *Procedia CIRP* 107 (2022) 15–20, <https://doi.org/10.1016/j.procir.2022.04.003>.
- [105] C. Caelli, F. Tamburrino, C. Brondi, A.V. Razonale, A. Ballarino, S. Barone, Sustainability in healthcare sector: the dental aligners case, *Sustainability* 15 (2023), <https://doi.org/10.3390/su152416757>.
- [106] M. Ateeq, A. Akbar, M. Shafique, Advancing circular economy: Comparative analysis of recycled and virgin carbon fiber 3D printed composites on performance and eco-efficiency, *Polym. (Guildf.)* 317 (2025) 127865, <https://doi.org/10.1016/j.polymer.2024.127865>.
- [107] M. Mele, G. Pisaneschi, M. Ciotti, G. Campana, A. Zucchelli, M. Fiorini, Environmental drawbacks of lightweight design algorithms in material extrusion additive manufacturing: a case study, *J. Braz. Soc. Mech. Sci. Eng.* 45 (2023) 530, <https://doi.org/10.1007/s40430-023-04456-8>.
- [108] I. Bianchi, A. Forcellese, T. Mancia, M. Simoncini, A. Vita, Process parameters effect on environmental sustainability of composites FFF technology, *Mater. Manuf. Process.* 37 (2022) 591–601, <https://doi.org/10.1080/10426914.2022.2049300>.
- [109] Q. Zhang, A.Y. Davis, M.S. Black, Emissions and Chemical Exposure Potentials from Stereolithography Vat Polymerization 3D Printing and Post-processing Units, *ACS Chem. Health Saf.* 29 (2022) 184–191, <https://doi.org/10.1021/acs.chas.2c00002>.
- [110] D.A. Baguley, G.S. Evans, D. Bard, P.S. Monks, R.L. Cordell, Review of volatile organic compound (VOC) emissions from desktop 3D printers and associated health implications, *J. Expo. Sci. Environ. Epidemiol.* (2025), <https://doi.org/10.1038/s41370-025-00778-y>.
- [111] S. Park, W. Shou, L. Makatura, W. Matusik, K. (Kelvin) Fu, 3D printing of polymer composites: materials, processes, and applications, *Matter* 5 (2022) 43–76, <https://doi.org/10.1016/j.matt.2021.10.018>.
- [112] T.L. Zontek, B.R. Ogle, J.T. Jankovic, S.M. Hollenbeck, An exposure assessment of desktop 3D printing, *J. Chem. Health Saf.* 24 (2017) 15–25, <https://doi.org/10.1016/j.jchas.2016.05.008>.
- [113] P. Azimi, D. Zhao, C. Pouzet, N.E. Crain, B. Stephens, Emissions of ultrafine particles and volatile organic compounds from commercially available desktop three-dimensional printers with multiple filaments, *Environ. Sci. Technol.* 50 (2016) 1260–1268, <https://doi.org/10.1021/acs.est.5b04983>.
- [114] A. Väisänen, L. Alonen, S. Ylönen, M. Hyttinen, Organic compound and particle emissions of additive manufacturing with photopolymer resins and chemical outgassing of manufactured resin products, *J. Toxicol. Environ. Health A* 85 (2022) 198–216, <https://doi.org/10.1080/15287394.2021.1998814>.
- [115] E. Venkata Prathyusha, S.S. Gomte, H. Ahmed, A. Prabakaran, M. Agrawal, N. Chella, A. Alexander, Nanostructured polymer composites for bone and tissue regeneration, *Int. J. Biol. Macromol.* 284 (2025) 137834, <https://doi.org/10.1016/j.ijbiomac.2024.137834>.
- [116] A. Skubis-Sikora, A. Hudecki, B. Sikora, P. Wiczorek, M. Hermyt, M. Hreczka, W. Likus, J. Markowski, K. Siemianowicz, A. Kolano-Burian, P. Czekaj, Toxicological assessment of biodegradable poli-ε-caprolactone polymer composite materials containing hydroxyapatite, bioglass, and chitosan as potential biomaterials for bone regeneration scaffolds, *Biomedicines* 12 (2024), <https://doi.org/10.3390/biomedicines12091949>.
- [117] H. Romanowski, F.S. Bierkandt, A. Luch, P. Laux, Summary and derived Risk Assessment of 3D printing emission studies, *Atmos. Environ.* 294 (2023) 119501, <https://doi.org/10.1016/j.atmosenv.2022.119501>.